Published for SISSA by Springer

Received: October 9, 2024
Accepted: January 28, 2025
Published: March 28, 2025

A collinear shower algorithm for NSL non-singlet fragmentation

Melissa van Beekveld,[a] **Mrinal Dasgupta**,[b] **Basem Kamal El-Menoufi**,[c] **Jack Helliwell**,[d] **Pier Francesco Monni**[e] **and Gavin P. Salam**[d,f]

[a] *Nikhef, Theory Group, Science Park 105, 1098 XG, Amsterdam, The Netherlands*
[b] *Department of Physics & Astronomy, University of Manchester, Manchester M13 9PL, U.K.*
[c] *School of Physics and Astronomy, Monash University, Wellington Road, Clayton, VIC-3800, Australia*
[d] *Rudolf Peierls Centre for Theoretical Physics, Clarendon Laboratory, Parks Road, University of Oxford, Oxford OX1 3PU, U.K.*
[e] *CERN, Theoretical Physics Department, CH-1211 Geneva, 23, Switzerland*
[f] *All Souls College, University of Oxford, Oxford OX1 4AL, U.K.*

E-mail: mbeekvel@nikhef.nl, mrinal.dasgupta@manchester.ac.uk, basem.el-menoufi@monash.edu, jack.helliwell@physics.ox.ac.uk, pier.monni@cern.ch, gavin.salam@physics.ox.ac.uk

Abstract: We formulate a collinear partonic shower algorithm that achieves next-to-single-logarithmic (NSL, $\alpha_s^n L^{n-1}$) accuracy for collinear-sensitive non-singlet fragmentation observables. This entails the development of an algorithm for nesting triple-collinear splitting functions. It also involves the inclusion of the one-loop double-collinear corrections, through a z-dependent NLO-accurate effective $1 \to 2$ branching probability, using a formula that can be applied more generally also to future full showers with $1 \to 3$ splitting kernels. The specific NLO branching probability is calculated in two ways, one based on slicing, the other using a subtraction approach based on recent analytical calculations. We close with demonstrations of the shower's accuracy for non-singlet partonic fragmentation functions and the energy spectrum of small-R quark jets. This work represents an important conceptual step towards general NNLL accuracy in parton showers.

Keywords: Jets and Jet Substructure, Parton Shower

ArXiv ePrint: 2409.08316

https://doi.org/10.1007/JHEP03(2025)209

JHEP03(2025)209

Contents

1 Introduction

Recent years have seen extensive work by multiple groups towards the development of parton showers that achieve next-to-leading logarithmic (NLL) accuracy [1–15]. Broadly speaking, NLL accuracy implies control of terms $\alpha_s^n L^n$, where α_s is the strong coupling and L is the logarithm of the ratio of any pair of disparate scales.

One of the next frontiers is to develop NNLL accurate showers, with control of terms $\alpha_s^n L^{n-1}$. A critical ingredient is the incorporation of splitting functions beyond first order in the coupling [16–31]. However, on its own, higher accuracy of the splitting function is not sufficient to achieve higher logarithmic accuracy. Concentrating on final-state showers, one significant recent step has been the inclusion of double-soft corrections [30] in such a way as to achieve $\alpha_s^n L^{n-1}$ (next-to-single logarithmic — NSL) accuracy [32–34] for observables like the distribution of energy flow in any given limited angular region, and $\alpha_s^n L^{2n-2}$ for subjet multiplicities [35, 36]. Another has been the development of an understanding of the connections between the soft-collinear, large-angle soft and triple-collinear regions. Together these advances have enabled the PanScales parton shower project to achieve NNLL accuracy

JHEP03(2025)209

for global and non-global event shape observables in $Z \to q\bar{q}$ and $H \to gg$ processes [31] (for corresponding calculations at NNLL and beyond see e.g. refs. [37–58]). One advance that is still needed for general NNLL accuracy in parton showers is the full treatment of the triple-collinear region. Arguably this is the last major step for general final-state NNLL accuracy at leading colour aside from NNLL spin correlations. It is required, for example, for $\alpha_s^n L^{n-1}$ accuracy for phenomenologically important quantities such as fragmentation functions and many jet substructure observables. Observables of this class are common in collider physics and have been extensively studied in the literature (see e.g. [58–84]). Its inclusion in showers would also open the door to potential new methods for merging parton showers with NNLO calculations (see e.g. refs. [28, 85–90] for existing methods), because it would ensure that parton showers reproduce all divergences that appear up to and including order α_s^2. Several groups have explored the triple collinear region for parton showers, both in the final and initial state [20, 22–26], though so far there have been only limited tests of their implications for logarithmic accuracy [22].

In this work, we take an exploratory approach to the problem of achieving $\alpha_s^n L^{n-1}$ in the collinear final-state regime, with the ultimate perspective of porting the lessons that we learn into the context of full showers, notably those being developed in the PanScales project. In section 2, we establish how to include the Abelian part of $q \to qgg$ branching [91, 92] in a positive-definite, unit-weight shower formalism. In section 3, we identify how to treat virtual corrections [93–97], with a core formula whose applicability is wider than parton-shower logarithmic accuracy and that connects with the work of refs. [21, 24, 28]. Then in section 4 we use that formula to evaluate the resulting NLO-accurate branching probabilities specifically for $q \to qg$ splitting, in both slicing and subtraction approaches, the latter building on the work of refs. [75, 81]. Together, these ingredients are sufficient for us to demonstrate, in section 5, $\alpha_s^n L^{n-1}$ accuracy for two distinct observables, in the limit of a large number of colours: the non-singlet fragmentation function [62, 63] and the small-R inclusive non-singlet quark-jet momentum distribution, with comparisons to calculations from ref. [98].[1] We conclude in section 6 and also provide additional technical appendices.

2 Formulation of a non-singlet final-state collinear shower

Let us start by formulating a standard strongly ordered non-singlet collinear shower. It involves an ordering scale v and the iteration of $1 \to 2$ splitting steps, each at a successively smaller values of v. It is useful to introduce a generic real branching probability

$$d\mathcal{R}_{1\to 2}(v_i, z_i, \phi_i | v_{i-1}) = \frac{dv_i}{v_i} dz_i \frac{d\phi_i}{2\pi} \frac{\alpha_s(\mu)}{\pi} P_{qq}(z_i) \Theta(v_i < v_{i-1}) \,, \tag{2.1}$$

where v_i has dimensions of energy, e.g. a transverse momentum and we have included the ordering condition relative to a previous emission at scale v_{i-1}. The renormalisation scale μ is to be taken of the order of the transverse momentum of the emitted gluon, and the splitting function is given by

$$P_{qq}(z) = C_F \, p_{qq}(z), \quad \text{with} \quad p_{qq}(z) = \frac{1+z^2}{1-z} \,. \tag{2.2}$$

[1] A conjecture for the two-loop anomalous dimension for small radius jet evolution was previously made in ref. [71].

JHEP03(2025)209

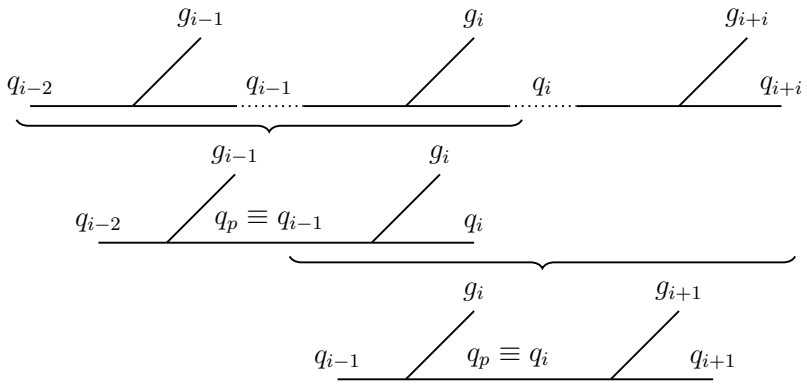

Figure 1. Cartoon illustration of how the shower builds up the $1 \to 3$ splitting functions from pairwise combinations of $1 \to 2$ splittings. The top line shows how the shower builds up a sequence of $1 \to 2$ splittings, while the second and third lines show how these are grouped and calculated using iterated $1 \to 3$ splitting functions. This cartoon ignores subtleties around unordered emissions and the freedom to choose the parent quark q_p. These subtleties are further discussed in the text and appendix A.1.

Then the distribution of branching i is given by

$$d\mathcal{P}_i = d\mathcal{R}_{1\to 2}(v_i, z_i, \phi_i \,|\, v_{i-1})\, \Delta(v_{i-1}, v_i) \,, \tag{2.3}$$

where the Sudakov form factor $\Delta(v_{i-1}, v_i)$ is specified through unitarity,

$$\Delta(v_{i-1}, v_i) = \exp\left[- \int d\mathcal{R}_{1\to 2}(v, z, \phi \,|\, v_{i-1})\, \Theta(v > v_i) \right] . \tag{2.4}$$

This is a standard formulation that guarantees single-logarithmic accuracy for collinear observables such as non-singlet fragmentation functions.

To achieve next-to-single logarithmic accuracy, we will need to modify the real branching probability so as to reproduce the full $1 \to 3$ matrix elements (and phase space) [91, 92]. We will also need to adjust the normalisation of splittings in the strongly ordered $1 \to 2$ limit so as to take into account the correct one-loop corrections to $1 \to 2$ splittings [93–97].

Let us first discuss how to incorporate the $1 \to 3$ splitting matrix element. We will concentrate on the abelian-like C_F^2, $q \to qgg$ contribution, as relevant for the non-singlet case.[2] Our approach will iterate $1 \to 2$ splittings, such that each step takes into account the kinematics and matrix element used to generate the prior $1 \to 2$ splitting and includes corrections such that the pair of splittings together has the correct $1 \to 3$ splitting matrix element. This is illustrated in figure 1. To be more specific, we concentrate on one specific pair of $1 \to 2$ splittings, which we label as

$$q_{i-2} \to g_{i-1}\, q_{i-1} \to g_{i-1}\, g_i\, q_i \,. \tag{2.5}$$

[2]For the full evaluation of the non-singlet fragmentation functions, in addition to $q \to qgg$ one also needs the non-trivial $(C_F(2C_F - C_A))$ part of the $q \to qq\bar{q}$, with identical flavours. In our numerical tests in section 5, we will work with colour factors chosen so that $C_A = 2C_F$, so that we can ignore this channel.

JHEP03(2025)209

Let us assume that the $q_{i-2} \to g_{i-1}\, q_{i-1}$ splitting has already been generated and was strongly ordered with respect to any prior splittings.[3] We will write the real splitting probability as the ratio of the full $1 \to 3$ splitting and phase space to the prior $1 \to 2$ splitting and phase space. First, for definiteness, it is useful to introduce the real phase space and matrix element for $1 \to 3$ splitting,

$$\left(\frac{\alpha_s}{\pi}\right)^2 \left(\frac{\mathrm{d}v_p}{v_p}\,\frac{\mathrm{d}\phi_p}{2\pi}\,\mathrm{d}z_p\right)\left(\frac{\mathrm{d}v_i}{v_i}\,\frac{\mathrm{d}\phi_i}{2\pi}\,\mathrm{d}z_i\right) p_{1\to3}(v_p, v_i, z_p, z_i, \phi_i - \phi_p)\,. \tag{2.6}$$

We have introduced the shorthand $p = i - 1$,[4] and we have

$$p_{1\to3}(v_p, v_i, z_p, z_i, \phi) = z_p\, x_{g_p} x_{g_i} x_{q_i} \frac{E^4\, \theta^2_{g_p q_p}\, \theta^2_{q_i g_i}}{s^2_{g_p g_i q_i}}\, C_F^2 \langle \hat{P}^{(\mathrm{ab})}_{q\to g_p g_i q_i}\rangle\,, \tag{2.7}$$

where E is the energy of the three parton system and $\langle \hat{P}^{(\mathrm{ab})}_{q\to g_p g_i q_i}\rangle$ corresponds to eq. (33) of ref. [92] (without any 1/2! symmetry factor). The energy fractions and invariant mass of the three particles involved in the triple-collinear spitting are parameterised as

$$x_{g_p} = 1 - z_p\,, \tag{2.8a}$$
$$x_{g_i} = z_p(1 - z_i)\,, \tag{2.8b}$$
$$x_{q_i} = z_p z_i\,, \tag{2.8c}$$
$$s_{ijk} = x_i x_j \theta^2_{ij} E^2 + \{i \leftrightarrow k\} + \{j \leftrightarrow k\}\,. \tag{2.8d}$$

Now we are in a position to write the probability for splitting i given a previous splitting p,

$$d\mathcal{R}_{2\to3}(v_i, z_i, \phi_i \,|\, p) = \frac{\alpha_s^{\mathrm{eff}}}{\pi}\left(\frac{\mathrm{d}v_i}{v_i}\,\frac{\mathrm{d}\phi_i}{2\pi}\,\mathrm{d}z_i\right)\frac{p_{1\to3}(v_p, v_i, z_p, z_i, \phi_i - \phi_p)}{P_{qq}(z_p)}\Theta(v_{g_i q_i} < v_{g_p q_i})\,, \tag{2.9}$$

where we return to the definition and functional dependence of the effective strength of emission, α_s^{eff}, below. An important consideration in eq. (2.9) is the replacement of the condition $v_i < v_{i-1}$ in eq. (2.1) with the condition $v_{g_i q_i} < v_{g_p q_i}$. Here v_{bc} is a kinematic variable defined in terms of the momenta of particles b and c (for example a relative transverse momentum), chosen so as to coincide with the ordering variable v for a splitting $a \to bc$. Thus $v_{g_i q_i}$ will coincide with v_i, but crucially $v_{g_p q_i}$ differs from $v_{g_p q_p} \equiv v_p$, because q_i will in general have a different momentum from q_p. A key relevant feature of the $v_{g_i q_i} < v_{g_p q_i}$ condition is that it is symmetric between the two gluons and therefore exactly accounts for the 1/2! symmetry factor that needs to be associated with the integral over the $1 \to 3$ phase space.[5] Note that $v_{g_p q_i}$ is known only after the generation of splitting i and that it can be either larger or smaller than v_p. Therefore, in the above approach, one must not additionally impose a $v_i < v_p$ condition. Instead, we start from $v_i = X v_p$, where X is large enough to ensure that the vast majority of the $v_{g_i q_i} < v_{g_p q_i}$ phase space is covered. Finally, note that the Sudakov factor in eq. (2.4) also needs to be modified to use eq. (2.9) in its integrand.

[3] At NSL accuracy, one need not worry about more than two consecutive commensurate-angle $1 \to 2$ splittings.

[4] Although it may be helpful to think of p as corresponding to $i - 1$ as in figure 1, this is not always the choice we make, as discussed in appendix A.1.

[5] In this context it would be interesting to explore the connections with the sectoring approach of ref. [28].

JHEP03(2025)209

Now we turn to α_s^{eff}. Assuming that v_i is a transverse-momentum like variable, then we can write

$$\alpha_s^{\text{eff}} = \alpha_s(v_i)\left[1 + \frac{\alpha_s(v_i)}{2\pi}K(z_i)\right] \tag{2.10}$$

where $K(z_i)$ generalises the well-known K_{CMW} [51, 99, 100] away from the soft limit. Its determination is discussed in sections 3 and 4. As we shall see in those sections, $K(z_i)$ diverges logarithmically when the quark becomes soft ($z_i \to 0$), which could cause α_s^{eff} to become negative. In practice therefore, we replace $\frac{\alpha_s(v_i)}{2\pi}K(z_i) \to \tanh\left(\frac{\alpha_s(v_i)}{2\pi}K(z_i)\right)$. A similar choice was made in refs. [30, 31], which is allowed because this replacement generates only additional terms beyond the nominal $\alpha_s^n L^{n-1}$ logarithmic accuracy.

Next, we set out our choice of ordering variable. We use

$$v_{g_i q_i} = \min(E_{g_i}, E_{q_i})\theta_{g_i q_i}\,, \tag{2.11}$$

which coincides with transverse momentum in the soft-gluon limit. Away from that limit one could have imagined a range of different choices, but not all are equally straightforward to implement within the above scheme.[6] A final comment that we make concerns a subtlety with the above picture connected with soft gluon emission. Specifically, while the intent of eq. (2.9) is to account for the $1 \to 3$ splitting function, there is a priori freedom in terms of which previously emitted gluon should be taken as the parent g_p. Simply taking the parent gluon to be $p = i - 1$ turns out to be incorrect and infrared unsafe. Instead we effectively take p to be that among all prior emissions that is closest in rapidity to i, with an additional prescription to avoid double-counting of phase-space regions. Appendix A.1 explains the issue and the details of our approach.

3 NLO-accurate inclusive emission probability

To understand how to calculate the $K(z)$ in eq. (2.10), it is helpful to consider a specific case, namely the emission of a collinear gluon g from an $e^+e^- \to q\bar{q}$ system. We will do this in two parts: we will consider the actual NLO cross section for producing a $q\bar{q}g$ system, inclusive over subsequent branchings from that system; separately we will consider the full shower expression for that gluon emission up to NLO, eq. (2.9); then we will determine $K(z)$ in eq. (2.10) by equating the actual NLO result and the shower's expansion to NLO. We will see that the result that emerges is independent of the specific choice of system (here $e^+e^- \to q\bar{q}$) that we took as our starting point, i.e. the process-dependent parts will cancel in $K(z)$.

We start with the first part. We take a Born matrix element and phase space $\bar{\alpha}B_{q\bar{q}g}d\Phi_{q\bar{q}g}$. Here, $\bar{\alpha} = \alpha_s(\mu)/2\pi$, with μ corresponding to the renormalisation scale, which should be taken of the order of the transverse momentum of the emitted gluon, as done explicitly in eq. (2.10). We use the convention of stripping out factors of $\bar{\alpha}$ from the various matrix elements. The NLO-corrected version of $B_{q\bar{q}g}$ will be written as $\bar{B}_{q\bar{q}g}$, with

$$\bar{\alpha}\bar{B}_{q\bar{q}g}d\Phi_{q\bar{q}g} = \bar{\alpha}B_{q\bar{q}g}d\Phi_{q\bar{q}g}\left(1 + \bar{\alpha}\frac{V_{q\bar{q}g}}{B_{q\bar{q}g}} + \bar{\alpha}\int_0^{\tilde{v}_g}\frac{d\Phi_{q\bar{q}ij}}{d\Phi_{q\bar{q}g}}\frac{B_{q\bar{q}ij}}{B_{q\bar{q}g}}\right), \tag{3.1}$$

[6] In particular, we also investigated $v_{g_i q_i} = E_{g_i}\theta_{g_i q_i}$, but found that this had problems with boundedness of eq. (2.9) in the limit where the p branching causes the quark q_p to become soft and the i branching causes the quark q_i to end up close in angle to g_p.

JHEP03(2025)209

where $V_{q\bar{q}g}$ is the one-loop correction to the $q\bar{q}g$ process, $B_{q\bar{q}ij}$ represents the matrix element for one further branching. The $\frac{d\Phi_{q\bar{q}ij}}{d\Phi_{q\bar{q}g}}$ factor represents the phase space in the exact shower map for one branching given the $q\bar{q}g$ starting point. There is an implicit sum over the possible final state channels $ij = \{gg, q\bar{q}\}$. The upper limit $\tilde{v}_g$ in the integration is to be understood as a shorthand for the ordering condition written in eq. (2.9) — or, more generally, the ordering condition in any shower that generates the correct $1 \to 3$ splitting functions.[7] Eq. (3.1) is the way the MC@NLO or POWHEG methods [101, 102] organise the NLO calculation given a Born $q\bar{q}g$ configuration.

Next consider the cross section that is obtained in the shower. A crucial assumption is that the shower is NLO accurate for the $q\bar{q}$ configuration, i.e. the starting point for the shower has a weight

$$\bar{B}_{q\bar{q}} d\Phi_{q\bar{q}} = B_{q\bar{q}} d\Phi_{q\bar{q}} \left(1 + \bar{\alpha}\frac{V_{q\bar{q}}}{B_{q\bar{q}}} + \bar{\alpha}\int_0^{v_{\max}} \frac{d\Phi_{q\bar{q}g}}{d\Phi_{q\bar{q}}}\frac{B_{q\bar{q}g}}{B_{q\bar{q}}}\right), \tag{3.2}$$

where the 0 to $v_{\max}$ limits on the integral indicate the range of allowed values of shower ordering variable v_g associated with the integration over the full g-emission phase space. The shower weight to obtain a $q\bar{q}g$ system is equal to

$$\bar{\alpha} S_{q\bar{q}g}\, d\Phi_{q\bar{q}g} = \bar{B}_{q\bar{q}}\, d\Phi_{q\bar{q}} \times \Delta(v_{\max}, v_g) \times \bar{\alpha}(1 + \bar{\alpha}K(z))\frac{d\Phi_{q\bar{q}g}}{d\Phi_{q\bar{q}}}\frac{B_{q\bar{q}g}}{B_{q\bar{q}}}\,, \tag{3.3}$$

where $K(z)$ is the shower NLO correction (to be determined) for the emission of a gluon with longitudinal momentum fraction $1 - z$ with respect to its emitter. The shower ordering variable at the point where the gluon is emitted has a value v_g. The Sudakov factor $\Delta(v_{\max}, v_g)$ is given by the unitary counterpart of the real emission probability

$$\Delta(v_{\max}, v_g) = \exp\left[-\int_{v_g}^{v_{\max}} \bar{\alpha}(1 + \bar{\alpha}K(z'))\frac{d\Phi_{q\bar{q}g'}}{d\Phi_{q\bar{q}}}\frac{B_{q\bar{q}g'}}{B_{q\bar{q}}}\right], \tag{3.4a}$$

$$= 1 - \bar{\alpha}\int_{v_g}^{v_{\max}} \frac{d\Phi_{q\bar{q}g'}}{d\Phi_{q\bar{q}}}\frac{B_{q\bar{q}g'}}{B_{q\bar{q}}} + \mathcal{O}\left(\bar{\alpha}^2\right). \tag{3.4b}$$

Putting together eqs. (3.2)–(3.4), and writing the result to relative order $\bar{\alpha}$ gives

$$\bar{\alpha} S_{q\bar{q}g}\, d\Phi_{q\bar{q}g} = \bar{\alpha} B_{q\bar{q}g} d\Phi_{q\bar{q}g}\left[1 + \bar{\alpha}\left(K(z) + \frac{V_{q\bar{q}}}{B_{q\bar{q}}} + \int_0^{v_g} \frac{d\Phi_{q\bar{q}g'}}{d\Phi_{q\bar{q}}}\frac{B_{q\bar{q}g'}}{B_{q\bar{q}}}\right) + \mathcal{O}\left(\bar{\alpha}^2\right)\right], \tag{3.5}$$

where we have combined the two integrals over $d\Phi_{q\bar{q}g}$.

Now we are ready to determine $K(z)$ by equating $\bar{\alpha}\bar{B}_{q\bar{q}g}$ and $\bar{\alpha}S_{q\bar{q}g}$ up to relative order $\bar{\alpha}$. This gives

$$K(z) = \frac{V_{q\bar{q}g}}{B_{q\bar{q}g}} - \frac{V_{q\bar{q}}}{B_{q\bar{q}}} + \int_0^{\tilde{v}_g} \frac{d\Phi_{q\bar{q}ij}}{d\Phi_{q\bar{q}g}}\frac{B_{q\bar{q}ij}}{B_{q\bar{q}g}} - \int_0^{v_g} \frac{d\Phi_{q\bar{q}g'}}{d\Phi_{q\bar{q}}}\frac{B_{q\bar{q}g'}}{B_{q\bar{q}}}\,. \tag{3.6}$$

[7] Given an ordering condition, and given that the initial gluon g is collinear, i and j will always be collinear and/or soft, as is required for the real phase space to be accurately generated with the triple collinear splitting function. Of course, the triple collinear splitting function does not generate the correct large-angle soft distribution, but as we shall see below, the contribution from this region cancels.

JHEP03(2025)209

There are important simplifications that can be made to eq. (3.6) thanks to the use of the collinear limit. Assuming that the gluon is collinear to the quark, ref. [97] has shown that

$$\frac{V_{q\bar{q}g}}{B_{q\bar{q}g}} - \frac{V_{q\bar{q}}}{B_{q\bar{q}}} = \frac{P_{qq}^{(1)}(s_{qg}, z, \epsilon, \mu^2)}{P_{qq}(z, \epsilon)}\,, \tag{3.7}$$

where $P_{qq}^{(1)}$ is a one-loop correction to the splitting function, which is independent of the hard process. We have made explicit that it depends on s_{qg} (the qg squared invariant mass), the dimensional regularisation parameter ϵ and the renormalisation scale μ. The bare expression for $P_{qq}^{(1)}$ is given in eq. (103) of ref. [97]. The renormalised expressions that we use are given in eq. (B.6). In dimensional regularisation, eq. (3.7) has a $1/\epsilon$ pole in the C_F and $T_R n_f$ colour factors and a $1/\epsilon^2$ divergence in the C_A colour factor.

Turning our attention now to the two real integrals of eq. (3.6), several comments are in order. Firstly, the $\tilde{v}_g$ and v_g upper bounds act on different phase spaces ($q\bar{q}g \to q\bar{q}ij$ and $q\bar{q} \to q\bar{q}g$ respectively) and so are not in general identical in the two real integrals. There is however one important region where they must coincide between the integrals. Consider, specifically the $ij = g_1 g_2$ channel in the left-hand integral. Labelling g_1 as the smaller-angle gluon, it concerns the situation where $\theta_{g_2 q} \gg \theta_{g_1 q}$, i.e. the angular anti-strong-ordered situation. Here the $\tilde{v}_g$ ordering condition on the $\{g_2, q\}$ phase space in the left-hand integral coincides with the v_g condition on the $\{g', q\}$ phase space in the right-hand integral. Furthermore, in this region, the two integrals will have identical integrands, because of the factorisation properties of the $q\bar{q}g_1g_2$ matrix element when one gluon (g_1) is collinear and the other (g_2, over which we integrate) is soft and at much larger angles. Therefore this region cancels between the two integrals. This is important, because it is the only region that carries dependence on the hard process, specifically when $\theta_{g_2 q}$ is of order 1. The cancellation ensures that the difference between the two integrals is process independent and that one is therefore free to replace the full matrix element with expressions involving just the universal $1 \to 2$ and $1 \to 3$ splitting functions. Together with the process-independence of eq. (3.7), this ensures that $K(z)$ as a whole does not depend on the process.

An important observation that we make is that a formula analogous to eq. (3.6) is valid for calculating the NLO-accurate emission probability generically for the n^{th} emission in any parton shower that had NLO accuracy for all prior emissions $1 \ldots (n-1)$. In particular, a similar form holds also for each of the nested soft and collinear gluon emissions that are the essence of the NLO-accurate parton branching kernel as needed for $\alpha_s^n L^{n-1}$ accuracy.[8]

Note that a formula essentially identical to eq. (3.6) has appeared in refs. [21, 24, 28] in the context of embedding NLO $Z \to 3\,\text{jets}$ within a shower that was already NLO accurate for $Z \to 2\,\text{jets}$. The presence of the same equation in both matching and shower kernels is significant because it implies that the infrared limit of $K(z)$ in matching will be by construction identical to the shower-kernel's $K(z)$ (so long as the treatment of real radiation

[8] Extending all of the ingredients beyond the collinear limit, such a formula is consistent also with the approach used in ref. [30]. One way of understanding that approach is to note that all terms in eq. (3.6) are independent of the soft gluon rapidity, except the first real integral. Exploiting the fact that K should agree with K_{CMW} in the soft-collinear limit, it is then straightforward to see that $K - K_{\text{CMW}}$ is given by the difference of that first real term between the situation with a soft gluon emitted at large angle and a soft-collinear emitted gluon. That is precisely the method used in ref. [30].

JHEP03(2025)209

is also the same between matching and shower). This property is precisely what was identified in ref. [103] as being crucial in order to maintain logarithmic accuracy when matching to fixed-order predictions and it suggests that eq. (3.6) and its counterparts in refs. [21, 24, 28] will play a major role in generalising logarithmically accurate matching beyond NLO.

As commented on above, the method that we have described relies crucially on having a shower that is NLO accurate for the process being studied. One interesting question for future research in the context of a full shower will be the interplay with approaches that provide NLO merging up to some multiplicity and LO accuracy beyond [104–109].

4 Evaluations of $K(z)$

4.1 C_F^2 term from a slicing scheme

One general way of evaluating eq. (3.6) is to apply a slicing scheme to the real integrals, splitting K into two parts

$$K(z) = K_<(z) + K_>(z)\,. \tag{4.1}$$

The first term contains the virtual corrections and the unresolved real contributions and needs to be evaluated using dimensional regularisation

$$K_<(z) = \frac{V_{q\bar{q}g}}{B_{q\bar{q}g}} - \frac{V_{q\bar{q}}}{B_{q\bar{q}}} + \int_0^{\tilde{\lambda}} \frac{d\Phi_{q\bar{q}ij}}{d\Phi_{q\bar{q}g}} \frac{B_{q\bar{q}ij}}{B_{q\bar{q}g}} - \int_0^{\lambda} \frac{d\Phi_{q\bar{q}g'}}{d\Phi_{q\bar{q}}} \frac{B_{q\bar{q}g'}}{B_{q\bar{q}}}\,. \tag{4.2a}$$

The second term is purely finite and reads

$$K_>(z) = \int_{\tilde{\lambda}}^{\tilde{v}_g} \frac{d\Phi_{q\bar{q}ij}}{d\Phi_{q\bar{q}g}} \frac{B_{q\bar{q}ij}}{B_{q\bar{q}g}} - \int_{\lambda}^{v_g} \frac{d\Phi_{q\bar{q}g'}}{d\Phi_{q\bar{q}}} \frac{B_{q\bar{q}g'}}{B_{q\bar{q}}}\,. \tag{4.2b}$$

The $\tilde{\lambda}$ and λ quantities represent the separation scales in the phase spaces of the two distinct real terms. As with the $\tilde{v}_g$ and v_g constraints, they need to act equivalently in the limit where $ij = g_1 g_2$ and $\theta_{g_2 q} \gg \theta_{g_1 q}$, in order to separately maintain the process independence of both $K_<(z)$ and $K_>(z)$. The physical scale associated with λ should be much smaller than the physical scale associated with v_g to ensure that λ/v_g suppressed power corrections are small.

In practice, for the abelian C_F^2 term, denoted by $K^{(\mathrm{ab})}$, we only need to consider the $ij = g_1 g_2$ channel.[9] We take g_2 to be the lower-v gluon and the conditions we apply in eqs. (4.2a) and (4.2b) are

$$\min(E_{g_2}, E_q)\theta_{g_2 q} \lesseqgtr \tilde{\lambda}\,, \tag{4.3a}$$

$$\min(E_{g'}, E_q)\theta_{g' q} \lesseqgtr \lambda\,, \tag{4.3b}$$

in analogy with the choice of ordering variable for our toy shower. One should keep in mind that the energy of the quark in the two conditions will in general be different. In the soft limit

[9] There is an additional C_F^2 contribution associated with the identical flavour $q \to q\bar{q}q$ splitting which is proportional to $C_F(2C_F - C_A)$. Our final results will be presented for $C_F = C_A/2$, eliminating this contribution.

JHEP03(2025)209

for g_2 and g', the conditions are, however, independent of the quark energy, and we obtain the process independence separately of both $K_<^{(\mathrm{ab})}(z)$ and $K_>^{(\mathrm{ab})}(z)$ by choosing $\tilde{\lambda} = \lambda$.[10]

The $K_<^{(\mathrm{ab})}(z)$ term is straightforward to evaluate analytically in dimensional regularisation. The details are provided in appendix B, with the slicing conditions of eq. (4.3) and $\tilde{\lambda}$ set equal to λ. The result is

$$K_<^{(\mathrm{ab})}(z) = 2C_F \left[\mathrm{Li}_2\left(-\frac{1-z}{z}\right) - \ln(z)\left(2\ln\frac{v_g}{\lambda} + \ln\frac{z(1-z)}{\min(1-z,z)^2}\right)\right] - \frac{C_F}{p_{qq}(z)}\,. \tag{4.4}$$

For the evaluation of $K_>^{(\mathrm{ab})}(z)$, we simply re-use the code developed for the toy shower as described in section 2, adapting it to carry out a single emission without a Sudakov form factor, i.e. operating it as a fixed-order code. In addition to the λ cutoff, we would also need to place a common cut on the maximum angle of any of i, j and g' so as to ensure that we remain in the collinear regime.

In practice, we find it is convenient to directly integrate the difference of the integrands, rather than to evaluate the two integrals separately. The cut on λ induces a term proportional to $\ln z \ln v_g/\lambda$ in $K_>^{(\mathrm{ab})}(z)$, which cancels against the corresponding term in $K_<^{(\mathrm{ab})}(z)$. That term dominates in the statistical errors for $K_>^{(\mathrm{ab})}(z)$, as in any slicing approach. To have better numerical behaviour, we instead directly evaluate a quantity

$$\bar{K}_>^{(\mathrm{ab})}(z) = K_>^{(\mathrm{ab})}(z) - 4C_F \ln z \ln\frac{v_g}{\lambda}\,, \tag{4.5}$$

using different choices of the large-angle cut in the $1 \to 2$ and $2 \to 3$ phase spaces, so as to subtract the logarithmic term. Specifically we match the logarithmic phase space volume between the two terms of eq. (4.2b) in the limit of strong v ordering. The results for $\bar{K}_>^{(\mathrm{ab})}(z)$ are shown in figure 2. We show several values of λ and, as expected, the dependence on λ becomes negligible as it is taken towards zero. We defer discussion of the structure of $K^{(\mathrm{ab})}(z)$ to section 4.3.

4.2 Relation of $K(z)$ with $\mathcal{B}_2^q(z)$ calculation

In this section, we will show how the quantity $K(z)$ can be simply related to the $\mathcal{B}_2(z)$ anomalous dimensions computed in refs. [75, 81]. In particular, for the NS flavour channel we will use the quark $\mathcal{B}_2^q(z)$ calculation of ref. [75]. For a quark, in the notation used for eq. (3.6) this quantity is defined as

$$\frac{\mathcal{B}_{2,v}^q(z)}{P_{qq}(z)} = \frac{V_{q\bar{q}g}}{B_{q\bar{q}g}} - \frac{V_{q\bar{q}}}{B_{q\bar{q}}} + \int_0^{\tilde{v}_g} \frac{d\Phi_{q\bar{q}ij}}{d\Phi_{q\bar{q}g}} \frac{B_{q\bar{q}ij}}{B_{q\bar{q}g}} - \int_0^{\tilde{v}_g} \left[\frac{d\Phi_{q\bar{q}ij}}{d\Phi_{q\bar{q}g}} \frac{B_{q\bar{q}ij}}{B_{q\bar{q}g}}\right]_{\text{s.o.}}\,. \tag{4.6}$$

The previous equation is a generalisation of the definition used in refs. [75, 81] to a generic ordering variable v, like that defined in eq. (2.11) (hence the v subscript). We see that the first three terms in eqs. (3.6) and (4.6) are in common, and the only difference, aside from normalisation, stems from the last term in the r.h.s. of eq. (4.6). In eq. (4.6), the term labelled

[10] If we had chosen invariant-mass conditions such as $E_{g_2} E_q \theta_{g_2 q} \lessgtr \tilde{\lambda}$ and analogously for the second condition, then we would lose the process independence unless we applied a suitable relative rescaling of the $\tilde{\lambda}$ and λ to take into account the different quark energies.

JHEP03(2025)209

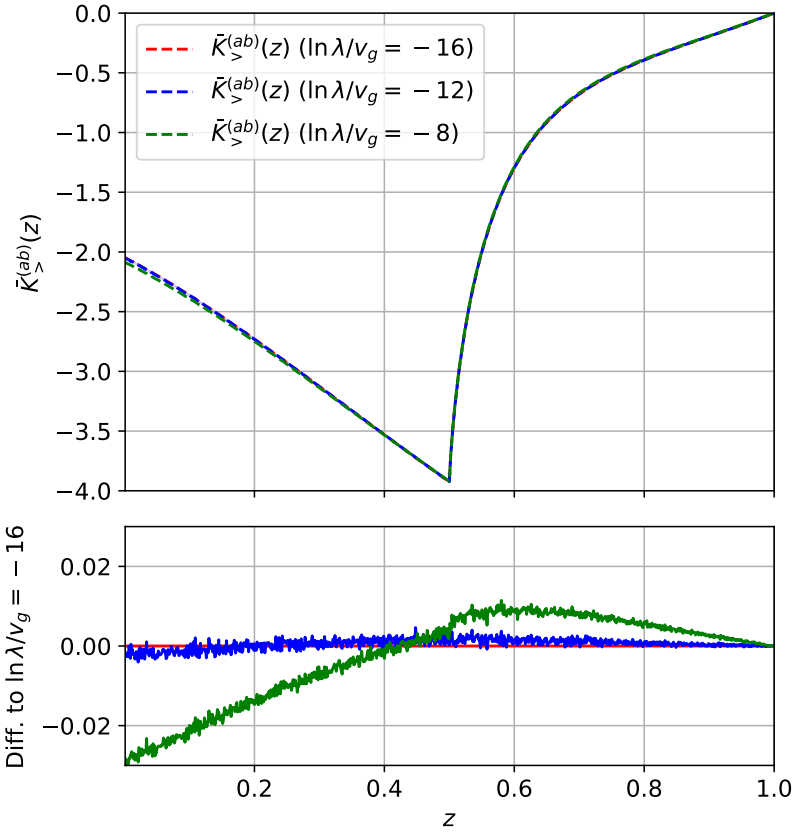

Figure 2. Top panel: Result for the $\bar{K}^{(\mathrm{ab})}_{>}$ slicing contribution, for three different choices of $\ln\lambda/v_g \in [-8, -12, -16]$. We set $C_F = 4/3$ for the numerical evaluations. Lower panel: Difference of $\bar{K}^{(\mathrm{ab})}_{>}$ evaluated with the above values of the cutoff to the result with $\ln\lambda/v_g = -16$.

by $[\dots]_{\mathrm{s.o.}}$ has the role of subtracting the strongly angular ordered approximation of the $1 \to 3$ splitting kernel entering the third term in the r.h.s. of the equation. In defining $\mathcal{B}^q_{2,v}(z)$ this is important so as to isolate NSL contributions arising solely from the commensurate-angles region of the $1 \to 3$ phase space.

We will start with the discussion of the C_F^2 colour channel and compare the result to what was obtained with the slicing scheme in the previous section. We will then discuss the $C_F C_A$, $C_F T_R n_f$, and $C_F(C_F - C_A/2)$ contributions (the latter will be eventually neglected by taking the large-N_c limit). In the discussion below, it is instructive to study first the simpler case of angular ordering, as originally considered in refs. [75, 81]. As we will show, for angular (θ) ordering the inclusive emission probability can be directly taken from these references, since the difference between $K(z)$ and $\mathcal{B}^q_2(z) \equiv \mathcal{B}^q_{2,\theta}(z)$ vanishes. We then move on to discuss the case of the ordering variable in eq. (2.11), used to obtain the numerical results of this article. In this case, additional considerations w.r.t. the angular ordering case are necessary, as will be discussed in the present section. As we will show, the quantity $K(z)$ is related to $\mathcal{B}^q_{2,v}(z)$ via a finite correction term involving only $1 \to 2$ splitting kernels, which can be computed in four space-time dimensions.

JHEP03(2025)209

4.2.1 Abelian C_F^2 contributions

We first connect $K(z)$ defined in eq. (3.6) and $\mathcal{B}_2^q(z)$ in the case of angular ordering, as initially considered in refs. [75, 81]. To avoid confusion, we will use $K_\theta(z)$ to denote $K(z)$ in eq. (3.6) obtained with angular ordering, while the notation $K(z)$ will be used for our default transverse-momentum ordering case.

Angular ordering case. The definition of $K_\theta(z)$ in eq. (3.6) can be easily related to $\mathcal{B}^q_{2,\theta}(z)$ in the C_F^2 channel ($\mathcal{B}^{q,C_F^2}_{2,\theta}(z)$), defined for instance in eq. (3.45) of ref. [75] and reported in appendix C (we remind the reader that the identical-quark splitting $q \to q\bar{q}q$, which would normally give a $C_F(C_F - C_A/2)$ contribution, is zero in the leading-N_c approximation that we use here). Aside from the overall normalisation factor $P_{qq}(z)$ mentioned above, the only difference between the two quantities is encoded in the last term of eq. (3.6) vs. the subtraction of the strongly-ordered contribution to $\mathcal{B}^q_{2,\theta}(z)$ in eq. (4.6) (see also eqs. (3.43) and (3.45) of ref. [75]). As stressed above, this term has the role of subtracting SL physics of strongly-ordered origin. Specifically, a first difference is that, in the calculation of $\mathcal{B}^{q,C_F^2}_{2,\theta}(z)$, the strongly-ordered subtraction is defined by integrating the product of leading-order splitting kernels with an ordering condition that coincides with the physical ordering, that is $\theta_{g_pq_i} > \theta_{g_iq_i}$. This corresponds to the $\tilde{v}_g$ physical ordering mentioned in section 3. Conversely, the calculation of the strongly-ordered subtraction in $K^{(\mathrm{ab})}_\theta(z)$ is performed with the shower ordering v_g, that in our case is equivalent to the condition $\theta_{g_pq_q} > \theta_{g_iq_i}$, where $\theta_{g_pq_p}$ is the angle between the first gluon and the intermediate quark that splits into g_iq_i. Secondly, while the strongly-ordered subtraction in the calculation of $\mathcal{B}^{q,C_F^2}_{2,\theta}(z)$ adopts the matrix element with collinear singularities given by $1/\theta^2_{g_pq_i} \times 1/\theta^2_{g_iq_i}$, the same ingredient in eq. (3.6) uses the shower matrix element with singularities $1/\theta^2_{g_pq_p} \times 1/\theta^2_{g_iq_i}$.

It is then clear that the difference between $\mathcal{B}^{q,C_F^2}_{2,\theta}(z)$ and $K^{(\mathrm{ab})}_\theta(z)$ is a term of strongly-ordered origin that is finite and can be calculated in four dimensions. We use the notation

$$\Delta\mathcal{B}^{q,C_F^2}_{2,\theta} \equiv \frac{P_{qq}(z)}{C_F^2} K^{(\mathrm{ab})}_\theta(z) - \mathcal{B}^{q,C_F^2}_{2,\theta}(z)\,, \tag{4.7}$$

to parameterise the difference from $K^{(\mathrm{ab})}_\theta(z)$ in the abelian colour channel. For angular ordering, an explicit calculation leads to

$$\begin{aligned}\Delta\mathcal{B}^{q,C_F^2}_{2,\theta} = p_{qq}(z) \Bigg(&\int \frac{d\theta^2_{g_pq_i}}{\theta^2_{g_pq_i}} \frac{d\theta^2_{g_iq_i}}{\theta^2_{g_iq_i}}\, dz_i \frac{d\Delta\phi}{2\pi}\, p_{qq}(z_i)\theta^2\delta(\theta^2 - \theta^2_{g_pq_i})\Theta(\theta_{g_pq_i} - \theta_{g_iq_i}) \\ &- \int \frac{d\theta^2_{g_pq_p}}{\theta^2_{g_pq_p}} \frac{d\theta^2_{g_iq_i}}{\theta^2_{g_iq_i}}\, dz_i \frac{d\Delta\phi}{2\pi}\, p_{qq}(z_i)\theta^2\delta(\theta^2 - \theta^2_{g_pq_p})\Theta(\theta_{g_pq_p} - \theta_{g_iq_i}) \Bigg) = 0\,.\end{aligned} \tag{4.8}$$

Here θ denotes the angle that is kept fixed in the definition of the Sudakov integrand, which corresponds to the shower evolution variable. In the first (second) integral, $\Delta\phi$ is the azimuthal angle between the plane containing g_p and q_i (q_p), and that containing g_i and q_i. Eq. (4.8) amounts to stating that, as demonstrated in refs. [75, 81], for an angular-ordered

JHEP03(2025)209

shower the quantity $\mathcal{B}_{2,\theta}^{q,C_F^2}(z)$ coincides (up to a normalisation) with $K_\theta^{(\mathrm{ab})}(z)$ needed for NSL accuracy. The explicit expression for $\mathcal{B}_{2,\theta}^{q,C_F^2}(z)$ is given in appendix C.

Transverse-momentum ordering case. We now switch to the case where the emissions are ordered in the transverse momentum variable defined in eq. (2.11). The quantity $\mathcal{B}_2^q(z)$ for this ordering variable in the abelian channel, $\mathcal{B}_{2,v}^{q,C_F^2}(z)$, can be expressed as (cf. appendix C)

$$\mathcal{B}_{2,v}^{q,C_F^2}(z) = \mathcal{B}_2^{q,\,\mathrm{an.},C_F^2}(z) + C_F^2 H_v^{\mathrm{fin.}}(z)\,. \tag{4.9}$$

The term $\mathcal{B}_2^{q,\,\mathrm{an.},C_F^2}(z)$ is the same as for angular ordering, first computed in ref. [75], and the result is reported in eqs. (C.6).

The quantity $H_v^{\mathrm{fin.}}(z)$ can instead be simply calculated numerically. Here we follow the same procedure used for the angular ordering case in refs. [75, 81], discussed in appendix C. One key property of $\mathcal{B}_2^q(z)$ is that it describes the physics of emissions at commensurate angles. In the explicit calculation, this requires the careful removal, from the triple-collinear splitting function, of the disparate angle configurations associated to single-logarithmic terms. In the transverse momentum ordering case, this subtraction involves removing both the sectors $\theta_{g_pq_i} \gg \theta_{g_iq_i}$ and $\theta_{g_pq_i} \ll \theta_{g_iq_i}$, which are allowed by the transverse momentum ordering condition $v_{g_pq_i} > v_{g_iq_i}$. This leads to a result for $H_v^{\mathrm{fin.}}(z)$ that reads[11]

$$\begin{aligned} H_v^{\mathrm{fin.}}(z) = \int d\Phi_3 (8\pi\alpha_s)^2 \Theta(v_{g_pq_i} - v_{g_iq_i})\,\delta(z - z_p)\,v\,\delta(v - v_{g_pq_i}) \\ \times \left(\frac{\langle P\rangle_{C_F^2}}{s_{g_pg_iq_i}^2} - \Theta(\theta_{g_pq_i} - \theta_{g_iq_i}) \left[\frac{\langle P\rangle_{C_F^2}}{s_{g_pg_iq_i}^2}\right]_{\theta_{g_pq_i} \gg \theta_{g_iq_i}} - \Theta(\theta_{g_iq_i} - \theta_{g_pq_i}) \left[\frac{\langle P\rangle_{C_F^2}}{s_{g_pg_iq_i}^2}\right]_{\theta_{g_pq_i} \ll \theta_{g_iq_i}} \right). \end{aligned} \tag{4.10}$$

The three-body phase space $d\Phi_3$ is explicitly defined in eq. (C.10) and the spin averaged $1 \to 3$ splitting function $\langle P\rangle_{C_F^2} = \langle P\rangle_{C_F^2}(x_{g_p}, x_{g_i}, x_{q_i})$ (with x_i being the longitudinal momentum fraction of particle i w.r.t. the energy of the initiating parton) can be found in ref. [92].

The two strongly-ordered counter-terms in the last line amount to subtracting the leading term in the expansion of $\frac{\langle P\rangle_{C_F^2}}{s_{g_pg_iq_i}^2}$ in the limits $\theta_{g_pq_i} \gg \theta_{g_iq_i}$ and $\theta_{g_pq_i} \ll \theta_{g_iq_i}$. This is crucial for $H_v^{\mathrm{fin.}}(z)$ to describe collinear dynamics at commensurate angles. Given our phase-space parametrisation (see also eq. (2.8))

$$x_{g_p} = 1 - z_p\,, \quad x_{g_i} = z_p\,(1 - z_i), \quad x_{q_i} = z_p\,z_i\,, \tag{4.11}$$

we obtain the following explicit expressions:

$$\left[\frac{\langle P\rangle_{C_F^2}}{s_{g_pg_iq_i}^2}\right]_{\theta_{g_pq_i} \gg \theta_{g_iq_i}} = \frac{\mathcal{J}_1(z_p, z_i)}{E^4}\,\frac{P_{qq}^{(0)}(1 - x_{g_p})}{\theta_{g_pq_i}^2}\,\frac{P_{qq}^{(0)}(1 - x_{g_i}/(1 - x_{g_p}))}{\theta_{g_iq_i}^2}\,, \tag{4.12}$$

$$\left[\frac{\langle P\rangle_{C_F^2}}{s_{g_pg_iq_i}^2}\right]_{\theta_{g_pq_i} \ll \theta_{g_iq_i}} = \frac{\mathcal{J}_2(z_p, z_i)}{E^4}\,\frac{P_{qq}^{(0)}(1 - x_{g_i})}{\theta_{g_pq_i}^2}\,\frac{P_{qq}^{(0)}(1 - x_{g_p}/(1 - x_{g_i}))}{\theta_{g_iq_i}^2}\,, \tag{4.13}$$

[11] For the angular ordering case, the analogous result is given in eq. (C.9), where the second term in brackets removes the configurations where $\theta_{g_pq_i} \gg \theta_{g_iq_i}$.

JHEP03(2025)209

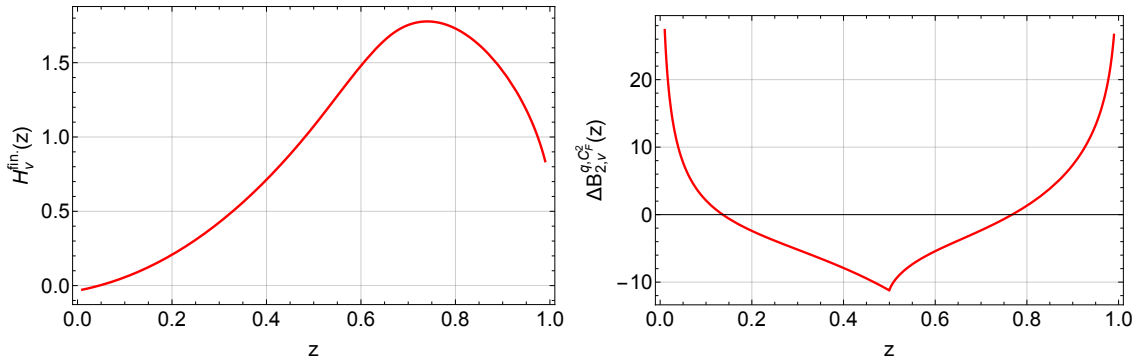

Figure 3. The functions $H_v^{\text{fin.}}(z)$ and $\Delta\mathcal{B}_{2,v}^{q,C_F^2}$.

where we defined

$$\mathcal{J}_1(z_p, z_i) \equiv \frac{1}{(1-z_p)z_p^3(1-z_i)z_i}, \tag{4.14}$$

$$\mathcal{J}_2(z_p, z_i) \equiv \frac{z_p}{1-z_p(1-z_i)}\mathcal{J}_1(z_p, z_i)\,. \tag{4.15}$$

We calculate eq. (4.10) numerically, and its result is shown in figure 3 (left).

As for the angular ordering case, the difference in the C_F^2 channel between $\mathcal{B}_{2,v}^{q,C_F^2}(z)$ and $K^{(\text{ab})}(z)$ amounts to an integral over the iterated $1 \to 2$ splitting function, while the genuine $1 \to 3$ contribution cancels between the two quantities. We then define

$$\Delta\mathcal{B}_{2,v}^{q,C_F^2} \equiv \frac{P_{qq}(z)}{C_F^2}K^{(\text{ab})}(z) - \mathcal{B}_{2,v}^{q,C_F^2}(z)\,. \tag{4.16}$$

The difference $\Delta\mathcal{B}_{2,v}^{q,C_F^2}$ stems from the different definition of the last term in the r.h.s. of eqs. (3.6), (4.6), and we calculate it analytically. Its expression is reported as an ancillary file with this article and it is shown in figure 3 (right). The plot shown in figure 4 demonstrates that the two calculations of $K^{(\text{ab})}(z)$ are in agreement at the per mil level.

Note that for the algorithm considered in this article, the shower-dependent quantity $\Delta\mathcal{B}_{2,v}^{q,C_F^2}$ depends only on strongly-ordered $1 \to 2$ splitting kernels, making it very simple to calculate. This may not be the case in general for other flavour channels, depending on the details of the implementation of the full $1 \to 3$ splitting in the shower.

4.2.2 Remaining colour channels

We now discuss the remaining channels contributing to $K(z)$ (3.6), including contributions from C_A, $T_R n_f$ and $C_F - C_A/2$ colour structures. A first aspect to consider is that $K(z)$ agrees with K_{CMW} [99] in the soft limit, that is

$$K(z) = K_{\text{CMW}} + \tilde{K}(z)\,, \tag{4.17}$$

where $\tilde{K}(z)$ vanishes in the soft limit and it is integrable in $z \in [0, 1]$. A second consideration is that, in the non-singlet channel considered here with $C_F = C_A/2$, the only flavour structures that modify the quark momentum are those related to consecutive independent (abelian)

JHEP03(2025)209

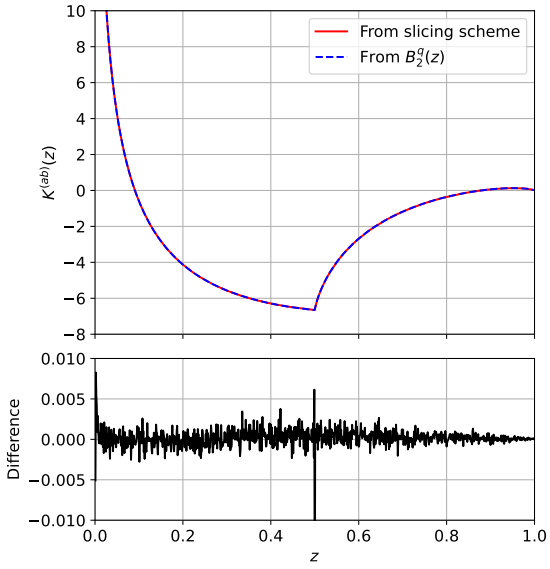

Figure 4. $K^{(\mathrm{ab})}(z)$ calculated both from the slicing scheme of section 4.1 and from $\mathcal{B}_{2,v}^{q,C_F^2}(z)$.

splittings, considered in the previous section. Therefore, in the NS channel, the contribution to $\tilde{K}(z)$ from splittings $q \to q\,p_1\,p_2$ not contributing to the abelian C_F^2 channel, can be obtained by fixing the kinematics of the parent $p_1 + p_2$ and integrating inclusively over the remaining phase space. This is precisely the definition of $\mathcal{B}_{2,v}^q$ given in appendix C. This gives a straightforward relationship between $\tilde{K}(z)$ and $\mathcal{B}_{2,v}^q$, which coincide, up to the usual $P_{qq}(z)$ normalisation, in the C_A, $T_R n_f$ and $C_F - C_A/2$ colour channels. This simple relationship will be modified once the non-abelian colour channels are included in the shower's $1 \to 3$ real radiation, as was the case for the C_F^2 contribution discussed in detail in the previous subsection. The methods presented in this article readily apply to those cases as well. Specific classes of observables, such as event shapes, are by construction not sensitive to the z dependence of $\mathcal{B}_{2,v}(z)$, but only to its inclusive integral. In these cases, a simplified procedure to relate the inclusive emission probability in the shower to the integral of $\mathcal{B}_{2,v}(z)$ was presented in ref. [31] in the context of NNLL-accurate parton showers.

4.3 Comments on structure of $K(z)$

Here we comment on the structure of the C_F^2 contribution to $K(z)$, as shown in figure 4. Firstly, we observe that $K(z)$ goes to zero for $z \to 1$. This is as expected, since at large z, the full $K(z)$ should reduce to the well known K_{CMW} term [99], which has C_A and $T_R n_f$ contributions, but no C_F contribution.

Secondly, it is continuous but not smooth at $z = 1/2$. In the slicing version of the calculation, such structure is explicitly seen in eq. (4.4), and is present also in $K_>(z)$. It connects with the use of a renormalisation scale choice $\mu = E\min(z, 1-z)\theta_{qg}$ and with the ordering condition in eqs. (2.9) and (2.11), both of which involve non-smooth behaviour at $z = 1/2$.

Next, we note that there is a $-C_F \ln^2(z)$ behaviour for $z \to 0$, which in the slicing calculations originates from $K_<^{(\mathrm{ab})}(z)$. This small-z integrable divergence was also already

JHEP03(2025)209

identified in $\mathcal{B}^{q,C_F^2}_{2,\theta}(z)$ in ref. [75]. The structure for $z \to 0$ is connected with the soft-quark limit and while interesting in its own right, goes beyond the scope of this article.

A crucial property of $\mathcal{B}_{2,v}(z)$ is that, analogously to its angular-ordered counterpart [75, 81], it satisfies the sum rule

$$\int_0^1 dz\, \mathcal{B}^q_{2,v}(z) = -\gamma_q + b_0 X_v\,, \tag{4.18}$$

where γ_q is the endpoint of time-like DGLAP anomalous dimension and the constant X_v depends on the chosen ordering variable, which can be easily obtained by integrating the expressions reported in appendix C. In the abelian channel this implies that $\mathcal{B}^q_{2,v}(z)$ should integrate to the corresponding C_F^2 term of $-\gamma_q$. This sum rule should not be modified by the contributions relating $\mathcal{B}^q_{2,v}(z)$ with $K(z)$, which we have verified is the case.

This is consistent with the expectations of ref. [31], specifically eqs. (3), (6) and (29). To help see this, it is useful to consider $\Delta_{\ln z}$ in eq. (6) of that reference (with z there corresponding to $1-z$ in this work). This quantity is the coefficient of a drift in $\ln(1-z)$ (using our notation) of a soft-collinear emission as induced by a subsequent splitting. In the soft-collinear limit, our shower leaves the kinematics of the soft-collinear gluon unchanged and therefore the drift is identically zero, and this results in the analogue of eq. (4.18) for $K(z)$. Note that the reason why one trivially has a zero drift here is that our real emission map preserves the kinematics of a first soft-collinear emission, while this is not the case for the full showers considered in ref. [31].

5 Logarithmic tests

Our implementation of the collinear shower does not include matching to NLO 2-jet production, which effectively corresponds to a coefficient function at the high scale. To test the shower, rather than starting the evolution from that high scale and including the corresponding coefficient function, we will consider the evolution between two disparate infrared scales and compare that result to a semi-analytic reference calculation obtained using a specifically adapted version of the HOPPET DGLAP evolution code [110], using the ingredients from refs. [63, 98]. We will carry out two sets of non-singlet tests, one on the fragmentation function, the other on the spectrum of small-R jets.

5.1 Non-singlet fragmentation function

We start by considering the non-singlet fragmentation function. In the collinear shower, this quantity is computed as follows. We start the shower evolution at a resolution scale $v_{\max}$, where the final state consists of a single quark of momentum fraction $z = 1$. We then evolve down to a second scale $v_{\min} \ll v_{\max}$, at which we measure the z distribution of the final quark.[12] We denote this quantity by $D^{(\mathrm{PS})}_{\mathrm{NS}}(z, v_{\min}, v_{\max})$.

To validate the shower result, we compare the resulting z distribution to a reference NSL calculation. Results at NSL for the fragmentation functions are known in the common $\overline{\mathrm{MS}}$

[12]The proper definition of the non-singlet fragmentation function would involve the difference in the z distribution between quarks and anti-quarks. However, since our proof-of-concept collinear shower does not contain $g \to q\bar{q}$ splittings, there are no anti-quarks in the final state.

JHEP03(2025)209

scheme, where the collinear singularities are regularised in $4-2\epsilon$ space-time dimensions. In order to connect to the shower result, we thus need to perform a scheme change, that can be implemented via a matching coefficient. Taking this into account, the analytic expectation for $D_{\rm NS}^{\rm (PS)}(z, v_{\rm min}, v_{\rm max})$ is given by

$$D_{\rm NS}^{\rm (NSL)}(z, v_{\rm min}, v_{\rm max}) = C(v_{\rm min}) \otimes \exp\left[\int_{v_{\rm min}^2}^{v_{\rm max}^2} \frac{dv^2}{v^2}\hat{P}(v)\right] \otimes C^{-1}(v_{\rm max})\,. \tag{5.1}$$

In the above equation, $\hat{P}(v) = \alpha_s(v)\hat{P}^{(0)}(z)/2\pi + \alpha_s^2(v)\hat{P}^{(1,\overline{\rm MS})}(z)/4\pi^2$ denotes the standard DGLAP non-singlet anomalous dimension in the $\overline{\rm MS}$ scheme [63] (the path ordering can be dropped in the non-singlet channel). The matching coefficient $C(v)$ encodes the scheme change from $\overline{\rm MS}$ to the shower regularisation scheme. At NSL, this is obtained by computing the order α_s contribution to the NS fragmentation function arising from the kinematical region below the shower cutoff. For the evolution variable defined in eq. (2.11), the NSL matching coefficient reads

$$C(v) \equiv \delta(1-z) + \frac{\alpha_s(v)}{2\pi}C^{(1)}(z) + \mathcal{O}(\alpha_s^2)\,, \tag{5.2}$$

where

$$\begin{aligned} C^{(1)}(z) = &-2\,P_{qq}(z)\left(\ln(1-z)\Theta\left(\frac{1}{2}-z\right) + z \leftrightarrow (1-z)\right) - C_F\,(1-z) \\ &- \frac{C_F}{6}\left(2\,\pi^2 - 3\,(7 - 6\,\ln 2)\right)\,\delta(1-z)\,. \end{aligned} \tag{5.3}$$

Eq. (5.1) thus converts the initial condition $\delta(1-z)$ from the shower scheme to $\overline{\rm MS}$ at the higher scale $v_{\rm max}$, it then evolves the resulting $\overline{\rm MS}$ fragmentation function down to $v_{\rm min}$, and finally it converts back to the shower scheme at the end of the evolution.

When comparing eq. (5.1) to the shower result, there will inevitably be subleading, NNSL, differences. To single out the pure SL and NSL contributions, we use a standard technique [2] which relies on a small-α_s limit, while holding fixed the variable

$$\lambda = \alpha_s(v_{\rm max})\ln\frac{v_{\rm min}}{v_{\rm max}}\,. \tag{5.4}$$

Specifically, we examine the quantity

$$\frac{D_{\rm NS}^{\rm (PS)}(z, v_{\rm min}, v_{\rm max})}{D_{\rm NS}^{\rm (NSL)}(z, v_{\rm min}, v_{\rm max})} - 1\,. \tag{5.5}$$

To test the SL accuracy of the collinear shower we can take the $\alpha_s \to 0$ limit of eq. (5.5). Similarly, the NSL accuracy can be tested by dividing Eq. (5.5) by α_s and then taking the $\alpha_s \to 0$ limit. In both cases, we expect the result to be consistent with zero.

The results of these SL and NSL accuracy tests are displayed in figure 5. As already explained in section 2, here we adopt the large-N_c limit in which we set $C_F = C_A/2 = 3/2$. In this limit, the contribution from the $q \to qq\bar{q}$ splitting (with identical flavours) vanishes. The left plot in figure 5 shows the fragmentation function $D_{\rm NS}^{\rm (PS)}(z, v_{\rm min}, v_{\rm max})$ for a set of small values of $\alpha_s \equiv \alpha_s(v_{\rm max})$. The right plots show the ratio eq. (5.5) (top panel) and the same

JHEP03(2025)209

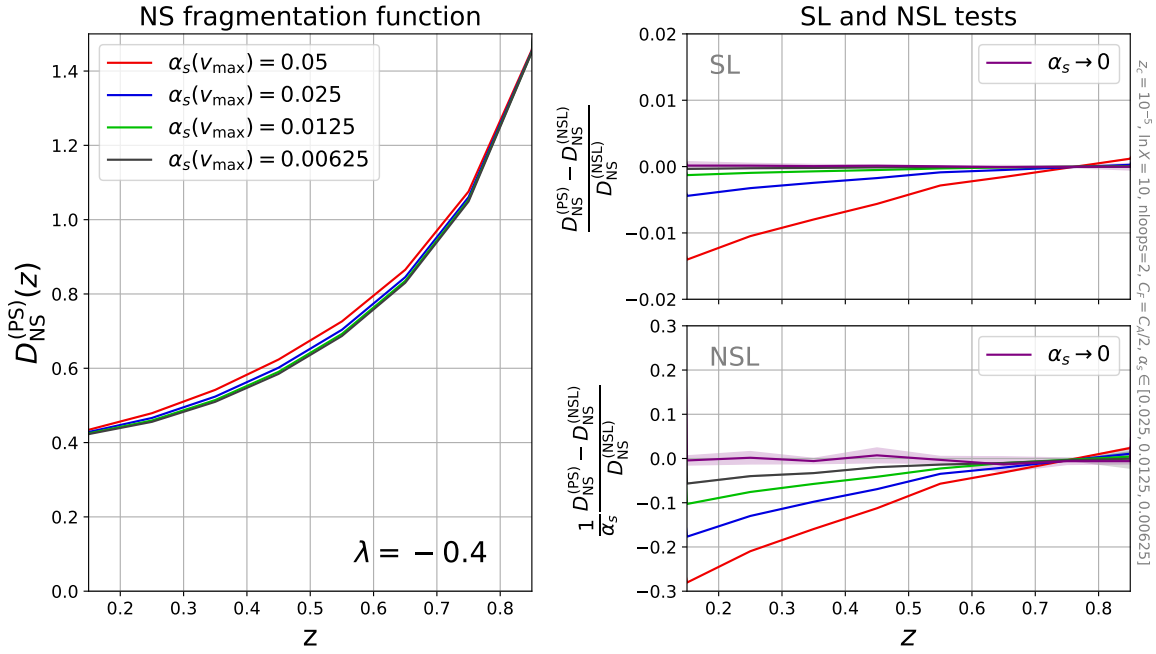

Figure 5. Shower non-singlet fragmentation function and associated logarithmic tests at $\lambda = -0.4$, cf. eq. (5.4). The left-hand panel shows the non-singlet fragmentation function as obtained with the collinear shower, for four values of the coupling. The upper-right panel shows a test of the shower's SL accuracy, where the $\alpha_s \to 0$ extrapolation gives a result consistent with zero, as expected for SL accuracy. The lower-right panel shows a test of the shower's NSL accuracy, illustrating that the $\alpha_s \to 0$ extrapolation is consistent with zero, as required for NSL accuracy.

quantity divided by α_s (bottom panel) for each of the above α_s values, and their extrapolation to $\alpha_s = 0$. In both cases, the extrapolated result agrees with zero to within statistical and extrapolation uncertainties, therefore showing consistency of the collinear shower with NSL accuracy. Additional technical details on the setup used in this test are given in appendix A.2.

To help appreciate the separate numerical impact of the triple-collinear and the inclusive NLO corrections, figure 6 shows the size of the NSL discrepancy that arises when various NSL contributions are turned off in the shower. The black curve corresponds to having just iterated $1 \to 2$ branchings (strictly ordered in the shower evolution variable v) and no inclusive $K(z)$ contribution. It demonstrates that the missing NSL terms can be up to $1.4 \times \alpha_s$, which would suggest missing effects of order 10−20% in a phenomenological context.[13] The green curve shows the result when one maintains the $1 \to 2$ structure but includes $K(z)$, while the blue curve uses the iterated $1 \to 3$ splitting, but without $K(z)$. These two curves show that the two sets of contributions are comparable in magnitude. The red curve includes all NSL contributions in the shower and is consistent with zero (it is identical to the purple curve of the lower-right panel of figure 5).

[13]The actual phenomenological impact in a specific full parton shower would depend on the structure of the uncontrolled NSL terms already generated by that shower. The study of this question is beyond the scope of this article, but ref. [31] showed in the context of event shapes that inclusion of correct NSL effects in full showers can indeed bring 10−20% corrections.

JHEP03(2025)209

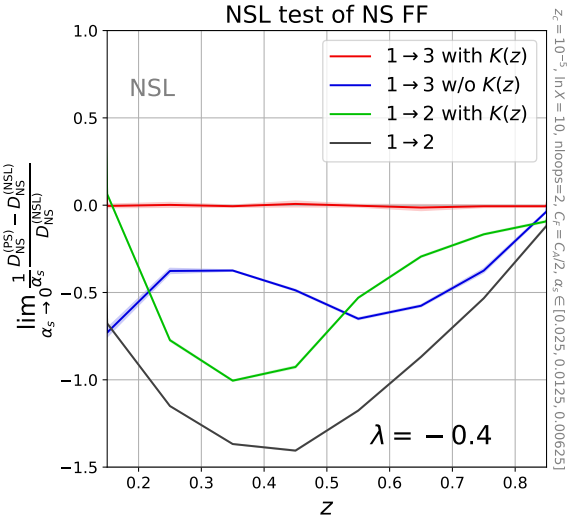

Figure 6. Illustration of the size of the NSL discrepancy in the non-singlet fragmentation function that arises when various NSL elements are left out. All curves already have the $\alpha_s \to 0$ limit taken.

5.2 Non-singlet small-R jets

Next, we consider an observable that is akin to the z spectrum of small-R jets inside a fat jet of radius R_0 and energy E, with $R \ll R_0 \ll 1$. We take a quark of energy E and start the shower evolution at a sufficiently high scale $v_{\max}$ such that for any $z \in [z_c, 1-z_c]$ the angular scale R_0 can be generated by the shower, where $z_c \ll 1$ is a cut-off on the splitting variable generated by the shower. Any emissions at angles larger than R_0 are vetoed, so as to mimic starting with a jet of radius R_0 and energy E, which can be thought of as an initial fragmentation function equal to $\delta(1-z)$. We continue the evolution down to a scale $v_{\min}$ such that for any $z \in [z_c, 1-z_c]$, the small angular scale R can be reached by the shower. This generates an ensemble of gluons plus one quark. We cluster that set of particles using the Cambridge/Aachen algorithm [111, 112] with jet radius R as implemented in FastJet [113]. We then identify the jet that contains the quark, and we histogram its momentum fraction z.[14] We refer to the resulting distribution as $D_{\mathrm{R}}^{(\mathrm{PS})}(z, ER, ER_0)$. Further technical details on the construction of the observable from the results of the collinear shower are given in appendix A.3.

The reference analytic calculation for this observable can be derived from existing work on microjet fragmentation functions [68, 71, 98]. At the NSL order, the result can be deduced from ref. [98], giving

$$D_{\mathrm{R}}^{(\mathrm{NSL})}(z, ER, ER_0) = C^{(R)}(ER) \otimes \exp\left[2\int_{ER}^{ER_0} \frac{d\mu}{\mu} \hat{P}^{(R)}(\mu, ER)\right] \otimes [C^{(R)}(ER_0)]^{-1}\,, \quad (5.6)$$

with

$$\hat{P}^{(R)}(\mu, E\,R) = \frac{\alpha_s(\mu^2)}{2\pi}\left(\hat{P}^{(0)}(z) + \frac{\alpha_s(\mu)}{2\pi}\hat{P}^{(1,\overline{\mathrm{MS}})}(z) - \frac{\alpha_s(ER)}{2\pi}\delta\hat{P}_{ik}^{(1)}\right)\,, \quad (5.7)$$

[14] Were our shower to include also $g \to q\bar{q}$ splittings, it would be necessary to use a jet algorithm that allows for an IRC-safe definition of jet flavour in the presence of soft-quark pairs [114–118], see also refs. [119–122] for related work.

JHEP03(2025)209

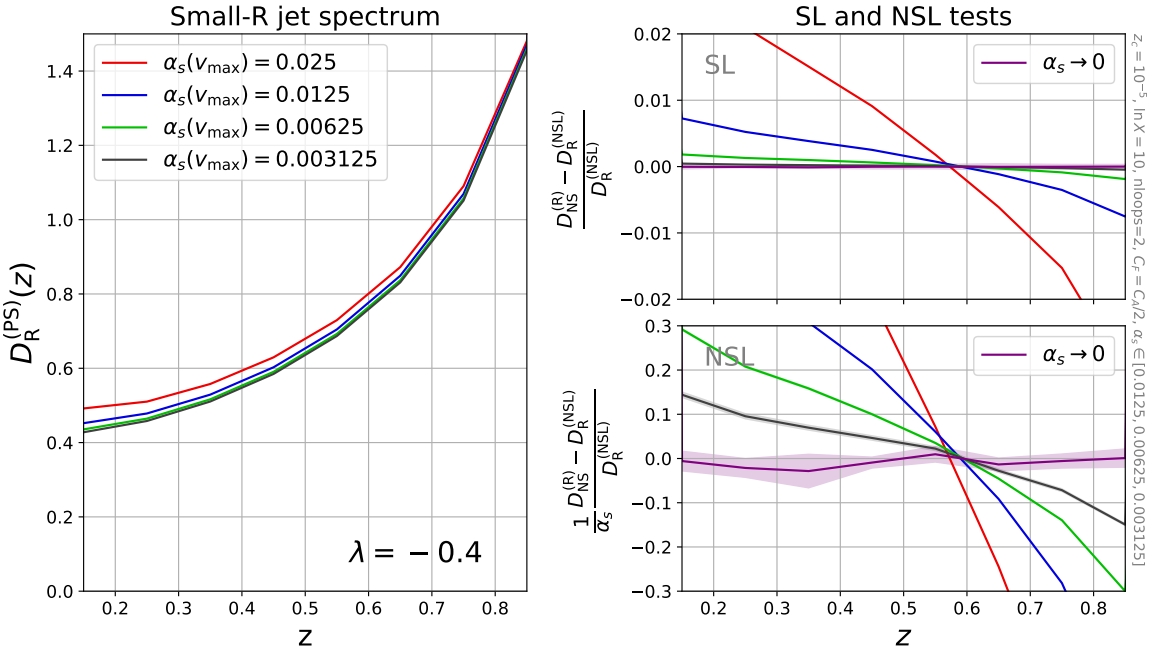

Figure 7. Shower small-R jet spectrum and associated logarithmic tests at $\lambda = -0.4$, cf. eq. (5.10). The left-hand panel shows the non-singlet small-R jet spectrum as obtained with the collinear shower, for four values of the coupling. The upper-right panel shows a test of the shower's SL accuracy, where the $\alpha_s \to 0$ extrapolation gives a result consistent with zero, as expected for SL accuracy. The lower-right panel shows a test of the shower's NSL accuracy, illustrating that the $\alpha_s \to 0$ extrapolation is consistent with zero, as required for NSL accuracy.

and

$$\delta\hat{P}_{qq}^{(1)}(z) \equiv \left(2\,\ln z\,\hat{P}_{qq}^{(0)}\right) \otimes \hat{P}_{qq}^{(0)} \tag{5.8a}$$

$$= -C_F^2\,\ln z\left(\frac{3\,z^2+1}{1-z}\ln z - 4\frac{1+z^2}{1-z}\ln(1-z) - \frac{z(4+z)+1}{1-z}\right). \tag{5.8b}$$

The coefficient function $C^{(R)}(\mu) = \delta(1-z) + \alpha_s(\mu)C^{(1,R)}(z)/2\pi$ involves

$$C^{(1,R)}(z) = -2\,C_F\,(1+z^2)\left(\frac{\ln(1-z)}{1-z}\right)_+ - C_F\left((1-z) + 2\frac{1+z^2}{1-z}\ln z\right)$$
$$+ C_F\left(\frac{13}{2} - \frac{2}{3}\pi^2\right)\delta(1-z)\,. \tag{5.9}$$

The main difference between eq. (5.6) and the expressions of ref. [98] is in the $[C^{(R)}(ER_0)]^{-1}$ factor, which accounts for the starting point of the shower, namely a jet of radius R_0 with energy E, as opposed to the NLO hard matching coefficient for $e^+e^- \to q\bar{q}$ that appears in ref. [98]. Recall that we consider only the non-singlet contributions, as in appendix C of that reference.

To test the shower, we use the same procedure as for the fragmentation function. Figure 7 (left) shows $D_R^{(PS)}(z, ER, ER_0)$, for $\lambda = \alpha_s(ER_0)\ln R/R_0 = -0.4$ for several values of

JHEP03(2025)209

$\alpha_s(ER_0)$. It looks quite similar to the left-hand plot of figure 5, as is to be expected given that the evolution of the two quantities is identical at SL level. Figure 7 (right) shows the comparison to eq. (5.6) as determined with HOPPET, examining the $\alpha_s \to 0$ limit of

$$\frac{D_{\mathrm{R}}^{(\mathrm{PS})}(z, ER, ER_0)}{D_{\mathrm{R}}^{(\mathrm{NSL})}(z, ER, ER_0)} - 1\,, \tag{5.10}$$

for the SL test (upper panel) and the $\alpha_s \to 0$ limit of the same quantity divided by α_s for the NSL test (lower panel). The $\alpha_s \to 0$ limits are consistent with zero in both cases, as is to be expected for an NSL-accurate collinear shower. It is a powerful test of the shower that it reproduces NSL accuracy both for the fragmentation function of section 5.1 and the small-R jet spectrum here.

6 Conclusions

In this article we have shown how to write a collinear shower that includes the Abelian part of the real $q \to qgg$ splitting function and the 1-loop corrections to $q \to qg$ splitting, so as to obtain $\alpha_s^n L^{n-1}$ accuracy for specific collinear fragmentation observables.

For the treatment of the real radiation, we made use of disordered emissions, where strict ordering in a shower evolution variable is replaced by strict ordering based on kinematics of the actual post-branching partons. This is the first use of such an approach in a study that aims for shower logarithmic accuracy beyond SL.

Our central equation for the treatment of virtual corrections is eq. (3.6), together with its simplifications in the collinear limit. Central to our approach is the treatment of virtual corrections through a consistent definition of the inclusive NLO probability associated with the underlying $1 \to 2$ shower splitting, as given in eq. (3.6). That equation demonstrates how to account for virtual corrections as an extension $K(z)$ of the standard soft K_{CMW} factor, generalised to be differential in the $1 \to 2$ splitting variables, but inclusive over subsequent branchings. Importantly, our approach can be applied to any shower algorithm. Section 4 showed concretely how to use eq. (3.6) in the collinear limit, using two independent methods for its evaluation, one based on a slicing approach and the other based on the approach and results of refs. [75, 81].

Since the shower is purely collinear, its scope is limited to observables that measure the energetic fragmentation products of a parton, specifically non-singlet flavour combinations (because of our inclusion, in the real part, of just $q \to qgg$ Abelian splittings). We examined two such observables, a partonic non-singlet fragmentation function and an inclusive small-R (quark) jet momentum distribution and confirmed that the shower reproduces known resummation results to $\alpha_s^n L^{n-1}$ accuracy.

This work, as part of a wider goal of general NNLL accuracy for full parton showers, provides important conceptual advances. In particular, the recent ref. [31] was able to achieve NNLL accuracy for event shape observables, in part by deducing $\int_0^1 dz[K(z) - K_{\mathrm{CMW}}]$ from elements of refs. [75, 81] and specific soft-collinear $1 \to 3$ and hard-collinear $1 \to 2$ characteristics of any given shower. The understanding developed here should instead make it possible to obtain the fully differential $K(z)$ in any given shower that includes triple-collinear

JHEP03(2025)209

real splittings. That will open the door to $\alpha_s^n L^{n-1}$ accuracy in full showers also for collinear fragmentation and a wide range of jet substructure observables. Finally we observe that some of the methods that we have explored here have connections with the merging of fixed-order calculations with parton showers, notably regarding the treatment of the virtual corrections in the approach of refs. [21, 24, 28]. As discussed recently [103], for matching to preserve logarithmic accuracy, it is critically important for the infrared limit of matching to coincide with the shower kernels, both in their treatment of the real and of the virtual corrections. We believe that further exploration of such connections has the potential to be highly fruitful for the formulation of logarithmically accurate matching beyond NLO.

Acknowledgments

We thank Keith Hamilton and Gregory Soyez for several discussions on the topics of this article and for insightful comments on the manuscript. We are also grateful to our other PanScales collaborators (Silvia Ferrario Ravasio, Alexander Karlberg, Ludovic Scyboz, Alba Soto-Ontoso, Silvia Zanoli) for various discussions on the underlying philosophy of the approach. We also thank each other's institutions for their hospitality at different stages of this project. This work has been funded by the European Research Council (ERC) under the European Union's Horizon 2020 research and innovation programme (grant agreement No. 788223, MD, BKE, JH, GPS) and under its Horizon Europe programme (grant agreement No. 101044599, PM), by a Royal Society Research Professorship (RP\R1\231001, GPS) and by the U.K.'s Science and Technologies Facilities Council under grants ST/T000864/1 (GPS), ST/X000761/1 (GPS), ST/T001038/1 (MD) and ST/00077X/1 (MD). In the last stages of the project, BKE has been supported by the Australian Research Council via Discovery Project DP220103512. Views and opinions expressed are however those of the authors only and do not necessarily reflect those of the European Union or the European Research Council Executive Agency. Neither the European Union nor the granting authority can be held responsible for them.

JHEP03(2025)209

A Technical details

In this appendix we discuss a number of technical aspects of the collinear shower implementation.

A.1 Parent-finding algorithm

The intent of the algorithm in section 2 is that if two gluons are emitted commensurate in angle and in energy (and far in angle or energy from any other gluon), then those two gluons should be produced with the full triple collinear splitting function. The question that we examine here is, for a given emission, how to choose the "parent" for use in the triple collinear splitting function. An example of the issue that needs to be addressed is illustrated in figure 8. Consider the emission of gluon $i = 3$ in that figure. The situation that is dangerous is that where gluons 1 and 3 are commensurate in angle and in energy (which implies $v_1 \sim v_3$), but there has been an intermediate emission 2, with $v_2 \sim v_3$, at much lower energy (much softer) and correspondingly at much larger angle. The issue is that if one uses a parent $p = i - 1$ $(= 2)$ then in the configuration that is shown, the triple

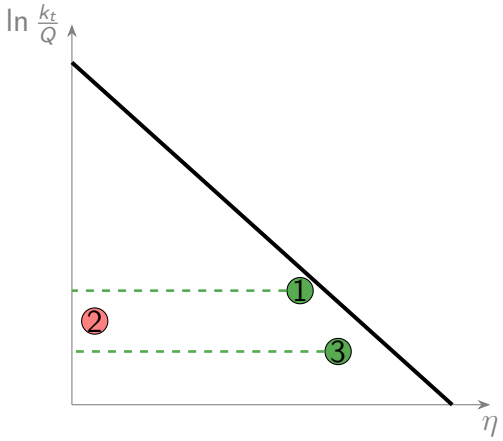

Figure 8. Lund diagram illustrating the IR safety issue that motivates need for a specific parent-finding algorithm. The fundamental issue is that when emitting 3, the correct set of partons to use in the triple collinear matrix element is 1 and 3. Naively using the emission immediately prior to 3, i.e. 2, would give an incorrect answer. See text for further details.

collinear correction would be applied to the $2,3$ combination. Because of strong angular ordering, that correction is simply equal to 1. Instead, it is the $1,3$ pair that requires a non-trivial correction, because of the proximity of 1 and 3 in angle. With $p = i - 1$, the presence of 2 would prevent the triple collinear correction from being applied to the $1,3$ pair. The probability of 2 being emitted between 1 and 3 is of the order of $\alpha_s \ln E_q/E_{\min} \ln v_1/v_3$, where $E_{\min}$ is a cutoff on the minimal allowed radiation energy. This is problematic because if one imagines an actual physical cutoff, $E_{\min} \sim k_t$, this implies $\alpha_s \ln E_q/E_{\min} \sim 1$, i.e. there would be an $\mathcal{O}(1)$ probability for the $1,3$ combination not to have the correct triple-collinear correction properly applied. This would break NSL accuracy. If instead one imagines taking $E_{\min}$ to be small, but with $\ln E_q/E_{\min}$ kept finite, then we would expect NSL accuracy to be retained, however one would have a spurious $\ln E_{\min}$ cutoff dependence appearing at NNSL.

To avoid this problem, we use the following "parent-finding" algorithm. Each emission j will be associated with a variable $v_p(j)$. When an emission is first created its $v_p(j)$ is set to infinity and we also store its angle θ_{jq} with respect to the quark at its time of creation. When a new emission i is trialled at a scale v, one determines the candidate parent p by identifying among all $j < i$ the one that has the smallest value of

$$\left| \ln \frac{\theta_{iq}}{\theta_{jq}} \right| . \tag{A.1}$$

This is effectively the prior emission that is closest in rapidity to i. If $v_p(p) > v$, then we use p to calculate the triple collinear correction. If $v_p(p) < v$, then we discard i and continue the shower evolution downwards from scale v. In either case, all $v_p(j)$ for $j < i$ are reset to $\min(v_p(j), v)$. Recall that if emission i is accepted, then we set $v_p(i) = \infty$.

To make the algorithm more concrete, and to help understand why it is correct, let us examine how it functions in two example configurations. Figure 9(a) shows a situation akin to that in figure 8. When emission 2 was created at scale v_2, $v_p(2)$ was set to ∞ and $v_p(1)$ to v_2 (shown by the horizontal dashed line). The vertical dashed line shows the separation

JHEP03(2025)209

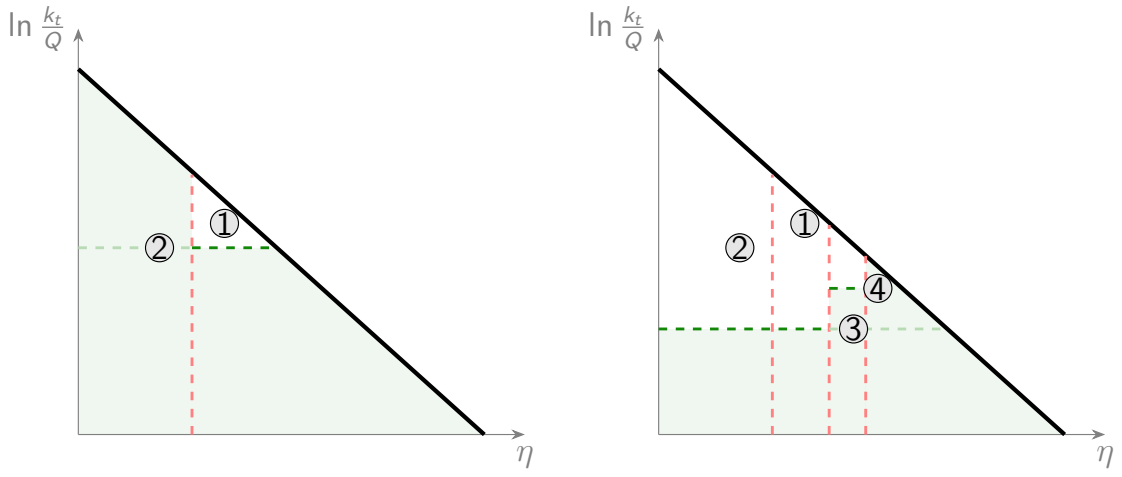

(a) (b)

Figure 9. Illustration of the parent-finding algorithm, (a) for a simple case and (b) for a more elaborate one. The shaded regions indicate where emissions are allowed, with the vertical dashed lines identifying the boundaries of rapidity regions that correspond to different parent choices. See text for further details.

into rapidities that are closer either to 2 or to 1. In the unshaded region, i.e. when closer in rapidity to 1 and when $v > v_p(1)$, then an attempted emission 3 will simply be discarded. If emission 3 is closer in rapidity to 1 but at a scale $v < v_p(1)$, then emission 3 will be trialled using a triple collinear matrix-element correction that involves 1 as a parent. Finally if emission 3 is closer in rapidity to 2, then emission 3 will be trialled with 2 as the parent, regardless of the value of v, because any value of v satisfies $v < v_p(2) = \infty$. This resolves the issue identified in figure 8. A more elaborate example is illustrated in figure 9(b), with the shaded area showing the region where emission 5 will be trialled, with the vertical lines showing the separation into the rapidity regions that determine the choice of parent.

A.2 Dependence on buffer and shower cutoffs

The aim of this section is to show that, for the algorithm of section 2 together with the parent-finding procedure detailed in section A.1, the results are independent (up to power corrections) of the technical parameters of the shower algorithm.

One technical parameter is $z_c \ll 1$ and it controls the maximum and minimum allowed gluon energies, $E_{\text{max}} = (1-z_c)E_q$ and $E_{\text{min}} = z_c E_q$. The other technical parameter is a buffer factor $X \gg 1$. Once an emission $i-1$ has occurred at a shower evolution scale v_{i-1}, the shower continues down not from $v = v_{i-1}$ but instead from $v = X v_{i-1}$. Note that the matrix element comes with a requirement that $\Theta(v_{g_i q_i} < v_{g_p q_i})$ (see eq. (2.9)), which together with our parent-finding algorithm ensures that we do not double-count emissions. The $X \to \infty$ limit ensures that all of the $v_{g_i q_i} < v_{g_p q_i}$ phase-space is covered.

In figure 10 we show the dependence of the spectrum of the NS fragmentation function

JHEP03(2025)209

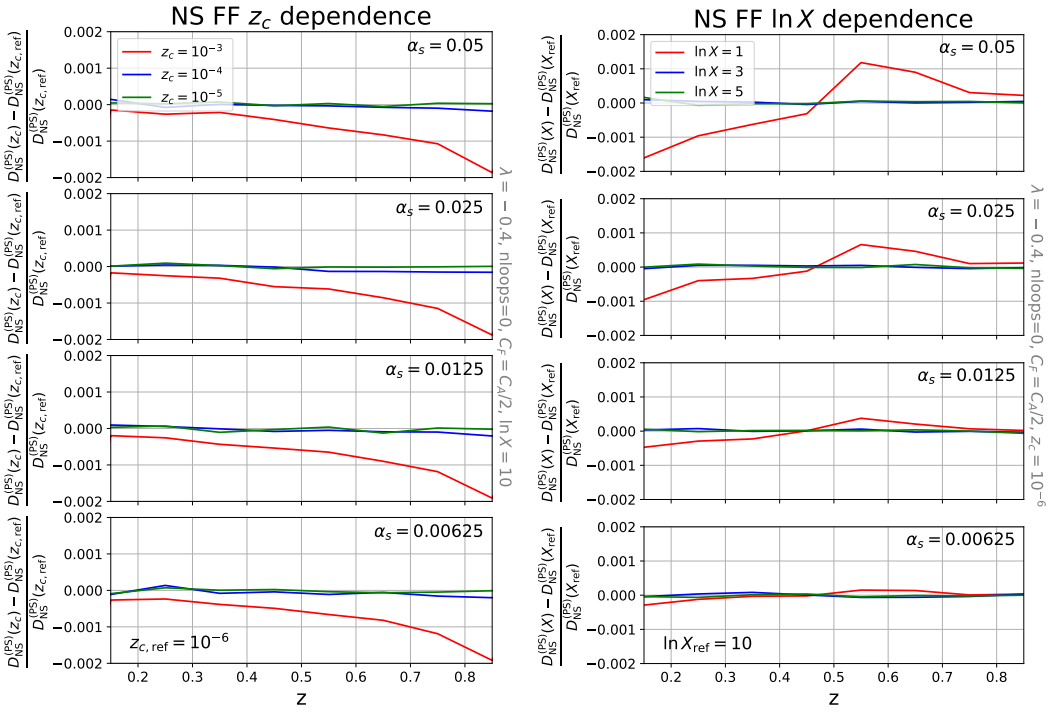

Figure 10. Test of z_c and buffer dependence of the NS fragmentation function for fixed coupling and $\lambda = -0.4$.

on z_c (left) and $\ln X$ (right) for several fixed α_s values through the quantity

$$\frac{D_{\mathrm{NS}}^{(\mathrm{PS})}(\delta) - D_{\mathrm{NS}}^{(\mathrm{PS})}(\delta_{\mathrm{ref}})}{D_{\mathrm{NS}}^{(\mathrm{PS})}(\delta_{\mathrm{ref}})}, \tag{A.2}$$

where $\delta = z_c$ or X and we have omitted the z, v_{min} and v_{max} dependence of $D_{\mathrm{NS}}^{(\mathrm{PS})}$ for brevity. As a reference value we take $z_c = 10^{-6}$ and $\ln X = 10$. We see that the result indeed tends to 0 as long as the energy cutoff is taken small enough ($z_c \lesssim 10^{-4}$), and the buffer size is taken large enough ($\ln X \gtrsim 3$). For all of the main results in this paper we have taken $z_c = 10^{-5}$ and $\ln X = 10$.

A.3 Treatment of relative angles during the shower evolution

The problem that we address here is we need to apply jet clustering in a limit where the angular separations between particles are very small. We work in double precision, i.e. numbers are stored to a relative precision of $\epsilon \sim 10^{-16}$. The difficulty we face is that two particles may be closer in angle than ϵ, in which case rounding errors could cause the jet clustering to follow the wrong sequence. To work around this difficulty we use the procedure described below.

We recall that the collinear phase-space is organised such that for each new gluon emission g_i we store its energy $E_i \equiv E_p(1 - z_i)$ (with E_p being the quark energy prior to the gluon emission), a polar angle $\theta_{g_i q_i}$ and an azimuthal angle $\Delta\phi$. Here $\Delta\phi$ is defined as the angle between the plane spanned by the parent splitting with its emitted gluon (g_p) and quark (q_p), and that by the decay products of that parent quark (q_i and g_i). We then retrieve the energy

JHEP03(2025)209

fraction and opening angle of the parent splitting, z_p and $\theta_{g_p q_p}$. The calculation of the small-R jet spectrum is sensitive to the relative angular distance between two emissions, meaning that we need a way to store correctly the angular distances between all emissions. The collinear shower's ordering variable is $v_p = \min[z_p, 1-z_p]\theta_{g_p q_p}$, hence smaller angle emissions do not necessarily come after large angle emissions. In addition, the collinear shower is not constructing actual four-momenta, but rather only their collinear counterparts. Therefore, care needs to be taken such that the correct angular distances between the emissions can be obtained. We adopt the following solution. Using the variables defined above, we assign to each $1 \to 3$ emission triplet an angle defined in a 2D (x, y) plane

$$\vec{\theta}_{g_p} = \theta_{g_p q_p}(1, 0)\,, \tag{A.3a}$$

$$\vec{\theta}_{g_i} = -z_i\,\theta_{g_i q_i}\,(\cos\Delta\phi, \sin\Delta\phi)\ , \tag{A.3b}$$

$$\vec{\theta}_{q_i} = (1-z_i)\,\theta_{g_i q_i}\,(\cos\Delta\phi, \sin\Delta\phi)\ , \tag{A.3c}$$

$$\theta_{g_p g_i} = |\vec{\theta}_{g_p} - \vec{\theta}_{g_i}|\,, \quad \theta_{g_p q_i} = |\vec{\theta}_{g_p} - \vec{\theta}_{q_p}|\,, \quad \theta_{g_i q_i} = |\vec{\theta}_{g_i} - \vec{\theta}_{q_p}|\,. \tag{A.3d}$$

When accepting the emission of the new g_i gluon, we subtract $\vec{\theta}_{q_i}$ from all emissions and from $\vec{\theta}_{q_i}$ itself. This aligns the final-state quark with the z axis with $\vec{\theta}_{q_i} = (0, 0)$. We moreover align $\vec{\theta}_{g_i}$ with the x axis before the next generation step. This makes sure that the correct relative angular distances between the accepted gluon emissions can be obtained.

After the shower has terminated, we create massless four-momenta using the stored energy E_i and $\vec{\theta}_i$ and

$$p_i = E_i\,(\sin\theta_i\cos\phi_i, \sin\theta_i\sin\phi_i, \cos\theta_i; 1)\,, \tag{A.4}$$

with $\theta_i = |\vec{\theta}_i|$ and $\phi_i = \arg(\vec{\theta}_i)$. These four-momenta are used as input to the clustering algorithm.

B Evaluating $\boldsymbol{K}_{<}^{(\mathbf{ab})}(\boldsymbol{z})$

In this section we show how to evaluate eq. (4.2a), using dimensional regularisation, in the limit of emissions being collinear to the quark. We focus on the case where $i, j = g_p, g_i$, with g_p having the larger v_g. We use the shower phase space and map as parameterised in eq. (2.8). In the limit that the slicing parameter $\lambda(\tilde{\lambda}) \ll v_g(\tilde{v}_g)$ we make use of the fact that the matrix elements and the phase space factorise. We can therefore write

$$\begin{aligned}\frac{d\Phi_{q\bar{q}g_1g_2}}{d\Phi_{q\bar{q}g}}\frac{B_{q\bar{q}g_1g_2}}{B_{q\bar{q}g}} = \frac{e^{\epsilon\gamma_{\mathrm{E}}}\Gamma(1-\epsilon)}{\Gamma(1-2\epsilon)}P_{qq}(z_i,\epsilon)\,\delta\left(\left(\frac{v_g}{E\min(z_p,1-z_p)}\right)^2 - \theta^2_{g_pq_p}\right)\\ \times\,\delta(z-z_p)(z_pz_i(1-z_i))^{-2\epsilon}\sin\Delta\phi^{-2\epsilon}dz_p dz_i\,d\theta^2_{g_pq_p}\frac{d\theta^2_{g_iq_i}}{\theta^{2+2\epsilon}_{g_iq_i}}\frac{d\Delta\phi}{2\pi}\end{aligned} \tag{B.1a}$$

and

$$\frac{d\Phi_{q\bar{q}g'}}{d\Phi_{q\bar{q}}}\frac{B_{q\bar{q}g'}}{B_{q\bar{q}}} = \frac{e^{\epsilon\gamma_{\mathrm{E}}}}{\Gamma(1-\epsilon)}P_{qq}(z_p,\epsilon)(z_p(1-z_p))^{-2\epsilon}dz_p\,\frac{d\theta^2_{g'q}}{\theta^{2+2\epsilon}_{g'q}}\,. \tag{B.1b}$$

JHEP03(2025)209

Here we have used

$$P_{qq}(z,\epsilon) = C_F\left(\frac{1+z^2}{1-z} - \epsilon(1-z)\right). \tag{B.2}$$

These are to be integrated in $v_{g_iq_i} = [0,\lambda]$ and $v_{g'q} = [0,\lambda]$ respectively (see eqs. (4.2a), (4.3)), recalling that we take $\tilde{\lambda} = \lambda$ as per section 4.1. We decide to write these phase-space constraints as

$$\Theta(\lambda > \min(E_{g_i}, E_{q_i})\theta_{g_iq_i}) = 1 - \Theta(\lambda/E < z_p \min(z_i, 1-z_i)\theta_{g_iq_i}), \tag{B.3a}$$

$$\Theta(\lambda > \min(E_{g'}, E_q)\theta_{g'q}) = 1 - \Theta(\lambda/E < \min(z_p, 1-z_p)\theta_{g'q}), \tag{B.3b}$$

such that there is one integral to be carried out in $4-2\epsilon$ dimensions, while the two other integrals involving a phase space constraint are finite in 4 dimensions. We then perform the integrals over $\Delta\phi$ and $\theta_{g_pq_p}$ in eq. (B.1a) and perform a change-of-variables to $z_i, \theta_{g_iq_i} \to z', \theta'$ for eq. (B.1a), and $z_p, \theta_{g'q} \to z', \theta'$ for eq. (B.1b) so as to bring the two integrands in a common form. After this the two real contributions of eq. (4.2a) can be written as

$$\begin{aligned}
\int_0^{\tilde{\lambda}} \frac{d\Phi_{q\bar{q}ij}}{d\Phi_{q\bar{q}g}} \frac{B_{q\bar{q}ij}}{B_{q\bar{q}g}} - \int_0^{\lambda} \frac{d\Phi_{q\bar{q}g'}}{d\Phi_{q\bar{q}}} \frac{B_{q\bar{q}g'}}{B_{q\bar{q}}} = \\
+ \int_0^{\theta^2_{\max}} \frac{d\theta'^2}{\theta'^{2(1+\epsilon)}} \int_0^1 dz' P_{qq}(z',\epsilon) z'^{-2\epsilon}(1-z')^{-2\epsilon}\left(z^{-2\epsilon}-1\right) \\
- \int_0^{\theta^2_{\max}} \frac{d\theta'^2}{\theta'^2} \int_0^1 dz' P_{qq}(z') \Theta\left(z\min(z',1-z')\theta' > \lambda/E\right) \\
+ \int_0^{\theta^2_{\max}} \frac{d\theta'^2}{\theta'^2} \int_0^1 dz' P_{qq}(z') \Theta\left(\min(z',1-z')\theta' > \lambda/E\right).
\end{aligned} \tag{B.4}$$

The factor of $z^{-2\epsilon}-1$ on the second line originates in the difference between the three and two particle phase spaces in d dimensions, and gives rise to a single pole which cancels against a corresponding pole in the virtual corrections. The constraint on the maximum angle $\theta_{\max}$ ensures that we stay in the collinear regime.

The integrals in eq. (B.4) can be readily evaluated, and read

$$\int_0^{\tilde{\lambda}} \frac{d\Phi_{q\bar{q}ij}}{d\Phi_{q\bar{q}g}} \frac{B_{q\bar{q}ij}}{B_{q\bar{q}g}} - \int_0^{\lambda} \frac{d\Phi_{q\bar{q}g'}}{d\Phi_{q\bar{q}}} \frac{B_{q\bar{q}g'}}{B_{q\bar{q}}} = -2C_F \ln(z)\left(\frac{1}{\epsilon} - \ln\frac{\lambda^2}{E^2}\right). \tag{B.5}$$

The virtual corrections are (up to $\mathcal{O}(\epsilon)$ terms)

$$\frac{V_{q\bar{q}g}}{B_{q\bar{q}g}} - \frac{V_{q\bar{q}}}{B_{q\bar{q}}} = 2C_F\left(\frac{\ln(z)}{\epsilon} + \mathrm{Li}_2\left(\frac{z-1}{z}\right) - \ln\frac{s_{qg}}{E^2}\ln(z)\right) - \frac{C_F}{p_{qq}(z)}, \tag{B.6}$$

where we use $s_{qg} = z(1-z)v_g^2/\min(z,1-z)^2$. Together with eq. (B.5) we find the result given in eq. (4.4).

C Definition of $\mathcal{B}_2^q(x)$

In this appendix we outline the expression of the quantity $\mathcal{B}_2^f(z)$ defined in refs. [75, 81]. In particular, we limit ourselves to reporting the expressions for the quark case, $\mathcal{B}_2^q(z)$, since the present article focusses on the non-singlet flavour channel.

JHEP03(2025)209

In the notation of ref. [81], $\mathcal{B}_2^q(z)$ can be expressed as[15]

$$\mathcal{B}_2^q(z) = \mathcal{B}_2^{q,\,\text{an.}}(z) + C_F^2 H^{\text{fin.}}(z)\,, \tag{C.1}$$

where

$$\begin{aligned}\mathcal{B}_2^{q,\,\text{an.}}(z) = {}& C_F^2\,\mathcal{B}_2^{q,\text{an.},C_F^2}(z) + C_F C_A\,\mathcal{B}_2^{q,\text{an.},C_F C_A}(z) + C_F T_R n_f\,\mathcal{B}_2^{q,\text{an.},C_F T_R}(z) \\ & + C_F\left(C_F - \frac{C_A}{2}\right)\mathcal{B}_2^{q,\text{an.,id.}}(z)\,.\end{aligned} \tag{C.2}$$

The term $\mathcal{B}_2^{q,\text{an.,id.}}(z)$ is neglected in the results presented in this article, which adopt the leading-N_c limit, i.e. $C_F = C_A/2$. To simplify the notation we absorb the term $\mathcal{B}_1^q(z) b_0 \ln g^2(z)$ in eq. (2.10) of [81] into $\mathcal{B}_2^q(z)$. In contrast with the convention adopted in [81], where we set $g(z) = 1 - z$, this term multiplies now the whole splitting function to allow for the possibility to set $g(z) \neq 1 - z$ also in the soft term of the inclusive emission probability. In practice, we use $g(z) = 1 - z$ for the angular ordering case while the ordering variable defined in eq. (2.11) corresponds to using $g(z) = \min(z, 1 - z)$ in the scale of the coupling. The functions in eq. (C.2) read

$$\mathcal{B}_2^{q,\text{an.,\,id.}}(z) = 4z - \frac{7}{2} + \frac{5z^2 - 2}{2(1-z)}\ln z + \frac{1+z^2}{1-z}\left(\frac{\pi^2}{6} - \ln z \ln(1-z) - \text{Li}_2(z)\right)\,, \tag{C.3}$$

$$\begin{aligned}\mathcal{B}_2^{q,\text{an.},C_F T_R}(z) = {}& -b_0^{(n_f)} p_{qq}(z)\ln z + b_0^{(n_f)}(1-z) - K^{(1),n_f}(1+z) \\ & + 2\,b_0^{(n_f)}(1+z)\ln(1-z) + b_0^{(n_f)} p_{qq}(z)\ln(g^2(z))\,,\end{aligned} \tag{C.4}$$

$$\begin{aligned}\mathcal{B}_2^{q,\text{an.},C_F C_A}(z) = {}& -b_0^{(C_A)} p_{qq}(z)\ln z + b_0^{(C_A)}(1-z) + \frac{3}{2}\frac{z^2\ln z}{1-z} + \frac{1}{2}(2z-1) \\ & + p_{qq}(z)\left(\ln^2 z + \text{Li}_2\left(\frac{z-1}{z}\right) + 2\,\text{Li}_2(1-z)\right) - K^{(1),C_A}(1+z) \\ & + 2\,b_0^{(C_A)}(1+z)\ln(1-z) + b_0^{(C_A)} p_{qq}(z)\ln(g^2(z))\,,\end{aligned} \tag{C.5}$$

$$\mathcal{B}_2^{q,\text{an.},C_F^2}(z) = p_{qq}(z)\left(-3\ln z - 2\ln z\ln(1-z) + 2\,\text{Li}_2\left(\frac{z-1}{z}\right)\right) - 1\,, \tag{C.6}$$

where we have used the decomposition

$$K^{(1)} = \left(\frac{67}{18} - \frac{\pi^2}{6}\right) C_A - \frac{10}{9}\,T_R\,n_f \equiv K^{(1),C_A}\,C_A + K^{(1),n_f}\,T_R\,n_f\,, \tag{C.7}$$

for the two-loop coefficient of the physical coupling scheme and

$$b_0 = \frac{11}{6}\,C_A - \frac{2}{3}\,T_R\,n_f \equiv b_0^{(C_A)}\,C_A + b_0^{(n_f)}\,T_R\,n_f\,, \tag{C.8}$$

for the first coefficient of the QCD beta function b_0. The function $g(z)$ parameterises the scale of the running coupling used in the Sudakov factor. A crucial aspect of eq. (C.1) is that the quantity $\mathcal{B}_2^{q,\,\text{an.}}(z)$ is independent of the ordering variable, and the complete dependence on the ordering is encoded in $H^{\text{fin.}}(z)$.

[15] The function $\mathcal{B}_2^q(z)$ computed in ref. [75] is defined as the $\mathcal{B}_2^q(z)$ used here multiplied by $(\alpha_s/(2\pi))^2$.

JHEP03(2025)209

For the case of the ordering variable (2.11) this is defined in eq. (4.10), while in the angular-ordered case it is given by the integral

$$H_\theta^{\text{fin.}}(z) = \int d\Phi_3 (8\pi\alpha_s)^2 \left(\frac{\langle P \rangle_{C_F^2}}{s^2_{g_p g_i q_i}} - \left[\frac{\langle P \rangle_{C_F^2}}{s^2_{g_p g_i q_i}} \right]_{\theta_{g_p q_i} \gg \theta_{g_i q_i}} \right) \Theta(\theta_{g_p q_i} - \theta_{g_i q_i}) \times \delta(z - z_p)\, \theta^2 \delta(\theta^2 - \theta^2_{g_p q_i})\,, \tag{C.9}$$

where we adopt the notation of eqs. (4.11), (4.12), (4.14). The invariant mass of the three-particle collinear system is denoted by $s_{g_p g_i q_i}$. The spin averaged $1 \to 3$ splitting function $\langle P \rangle_{C_F^2} = \langle P \rangle_{C_F^2}(x_{g_p}, x_{g_i}, x_{q_i})$ (with x_i being the longitudinal momentum fraction of particle i w.r.t. the energy of the initiating parton) can be found in ref. [92], and $\left[\frac{\langle P \rangle_{C_F^2}}{s^2_{g_p g_i q_i}} \right]_{\theta_{g_p q_i} \gg \theta_{g_i q_i}}$ denotes the limit of the quantity $\frac{\langle P \rangle_{C_F^2}}{s^2_{g_p g_i q_i}}$ in the strongly ordered regime $\theta_{g_p q_i} \gg \theta_{g_i q_i}$, and it is given in eq. (4.12). Finally, the three-body phase space measure $d\Phi_3$, including the Jacobian factor for the chosen parametrisation, is given by (Δ denotes the Gram determinant, see refs. [75, 81])

$$d\Phi_3 \equiv \frac{z_p}{\pi} \frac{E^4}{(4\pi)^4} dz_p\, dz_i\, d\theta^2_{g_p q_i}\, d\theta^2_{g_i q_i}\, d\theta^2_{g_p g_i}\, (1 - z_p)\, z_p^2\, (1 - z_i)\, z_i\, \Delta^{-1/2}\, \Theta(\Delta)\,. \tag{C.10}$$

Eq. (C.9) can be reduced to a 1-fold integral (cf. figure 4 of ref. [75]), that is provided as an ancillary file with ref. [81]. The function $\mathcal{B}^q_{2,\theta}(z)$ is regular in the soft limit $z \to 1$ and is thus fully integrable over $z \in [0, 1]$.

Data Availability Statement. This article has no associated data or the data will not be deposited.

Code Availability Statement. This article has associated code in a code repository. Available at: https://zenodo.org/records/14976718.

References

[1] M. Dasgupta et al., *Logarithmic accuracy of parton showers: a fixed-order study*, *JHEP* **09** (2018) 033 [*Erratum ibid.* **03** (2020) 083] [arXiv:1805.09327] [INSPIRE].

[2] M. Dasgupta et al., *Parton showers beyond leading logarithmic accuracy*, *Phys. Rev. Lett.* **125** (2020) 052002 [arXiv:2002.11114] [INSPIRE].

[3] K. Hamilton et al., *Colour and logarithmic accuracy in final-state parton showers*, *JHEP* **03** (2021) 041 [arXiv:2011.10054] [INSPIRE].

[4] A. Karlberg, G.P. Salam, L. Scyboz and R. Verheyen, *Spin correlations in final-state parton showers and jet observables*, *Eur. Phys. J. C* **81** (2021) 681 [arXiv:2103.16526] [INSPIRE].

JHEP03(2025)209

[5] K. Hamilton et al., *Soft spin correlations in final-state parton showers*, *JHEP* **03** (2022) 193 [arXiv:2111.01161] [INSPIRE].

[6] M. van Beekveld et al., *PanScales parton showers for hadron collisions: formulation and fixed-order studies*, *JHEP* **11** (2022) 019 [arXiv:2205.02237] [INSPIRE].

[7] M. van Beekveld et al., *PanScales showers for hadron collisions: all-order validation*, *JHEP* **11** (2022) 020 [arXiv:2207.09467] [INSPIRE].

[8] M. van Beekveld and S. Ferrario Ravasio, *Next-to-leading-logarithmic PanScales showers for Deep Inelastic Scattering and Vector Boson Fusion*, *JHEP* **02** (2024) 001 [arXiv:2305.08645] [INSPIRE].

[9] J.R. Forshaw, J. Holguin and S. Plätzer, *Building a consistent parton shower*, *JHEP* **09** (2020) 014 [arXiv:2003.06400] [INSPIRE].

[10] Z. Nagy and D.E. Soper, *Summations by parton showers of large logarithms in electron-positron annihilation*, arXiv:2011.04777 [INSPIRE].

[11] Z. Nagy and D.E. Soper, *Summations of large logarithms by parton showers*, *Phys. Rev. D* **104** (2021) 054049 [arXiv:2011.04773] [INSPIRE].

[12] F. Herren et al., *A new approach to color-coherent parton evolution*, *JHEP* **10** (2023) 091 [arXiv:2208.06057] [INSPIRE].

[13] B. Assi and S. Höche, *New approach to QCD final-state evolution in processes with massive partons*, *Phys. Rev. D* **109** (2024) 114008 [arXiv:2307.00728] [INSPIRE].

[14] C.T. Preuss, *A partitioned dipole-antenna shower with improved transverse recoil*, *JHEP* **07** (2024) 161 [arXiv:2403.19452] [INSPIRE].

[15] S. Höche, F. Krauss and D. Reichelt, *The Alaric parton shower for hadron colliders*, arXiv:2404.14360 [INSPIRE].

[16] K. Kato and T. Munehisa, *Monte Carlo Approach to QCD Jets in the Next-to-leading Logarithmic Approximation*, *Phys. Rev. D* **36** (1987) 61 [INSPIRE].

[17] K. Kato and T. Munehisa, *Double Cascade Scheme for QCD Jets in e^+e^- Annihilation*, *Phys. Rev. D* **39** (1989) 156 [INSPIRE].

[18] K. Kato and T. Munehisa, *NLLjet: A Monte Carlo code for e^+e^- QCD jets including next-to-leading order terms*, *Comput. Phys. Commun.* **64** (1991) 67 [INSPIRE].

[19] K. Kato, T. Munehisa and H. Tanaka, *Next-to-leading logarithmic parton shower in deep inelastic scattering*, *Z. Phys. C* **54** (1992) 397 [INSPIRE].

[20] S. Jadach, A. Kusina, M. Skrzypek and M. Slawinska, *Two real parton contributions to non-singlet kernels for exclusive QCD DGLAP evolution*, *JHEP* **08** (2011) 012 [arXiv:1102.5083] [INSPIRE].

[21] L. Hartgring, E. Laenen and P. Skands, *Antenna Showers with One-Loop Matrix Elements*, *JHEP* **10** (2013) 127 [arXiv:1303.4974] [INSPIRE].

[22] S. Jadach, A. Kusina, W. Płaczek and M. Skrzypek, *NLO corrections in the initial-state parton shower Monte Carlo*, *Acta Phys. Polon. B* **44** (2013) 2179 [arXiv:1310.6090] [INSPIRE].

[23] S. Jadach, A. Kusina, W. Płaczek and M. Skrzypek, *On the dependence of QCD splitting functions on the choice of the evolution variable*, *JHEP* **08** (2016) 092 [arXiv:1606.01238] [INSPIRE].

[24] H.T. Li and P. Skands, *A framework for second-order parton showers*, *Phys. Lett. B* **771** (2017) 59 [arXiv:1611.00013] [INSPIRE].

JHEP03(2025)209

[25] S. Höche and S. Prestel, *Triple collinear emissions in parton showers*, *Phys. Rev. D* **96** (2017) 074017 [arXiv:1705.00742] [INSPIRE].

[26] S. Höche, F. Krauss and S. Prestel, *Implementing NLO DGLAP evolution in Parton Showers*, *JHEP* **10** (2017) 093 [arXiv:1705.00982] [INSPIRE].

[27] F. Dulat, S. Höche and S. Prestel, *Leading-Color Fully Differential Two-Loop Soft Corrections to QCD Dipole Showers*, *Phys. Rev. D* **98** (2018) 074013 [arXiv:1805.03757] [INSPIRE].

[28] J.M. Campbell et al., *Towards NNLO+PS matching with sector showers*, *Phys. Lett. B* **836** (2023) 137614 [arXiv:2108.07133] [INSPIRE].

[29] L. Gellersen, S. Höche and S. Prestel, *Disentangling soft and collinear effects in QCD parton showers*, *Phys. Rev. D* **105** (2022) 114012 [arXiv:2110.05964] [INSPIRE].

[30] S. Ferrario Ravasio et al., *Parton Showering with Higher Logarithmic Accuracy for Soft Emissions*, *Phys. Rev. Lett.* **131** (2023) 161906 [arXiv:2307.11142] [INSPIRE].

[31] M. van Beekveld et al., *New Standard for the Logarithmic Accuracy of Parton Showers*, *Phys. Rev. Lett.* **134** (2025) 011901 [arXiv:2406.02661] [INSPIRE].

[32] A. Banfi, F.A. Dreyer and P.F. Monni, *Next-to-leading non-global logarithms in QCD*, *JHEP* **10** (2021) 006 [arXiv:2104.06416] [INSPIRE].

[33] A. Banfi, F.A. Dreyer and P.F. Monni, *Higher-order non-global logarithms from jet calculus*, *JHEP* **03** (2022) 135 [arXiv:2111.02413] [INSPIRE].

[34] T. Becher, N. Schalch and X. Xu, *Resummation of Next-to-Leading Nonglobal Logarithms at the LHC*, *Phys. Rev. Lett.* **132** (2024) 081602 [arXiv:2307.02283] [INSPIRE].

[35] R. Medves, A. Soto-Ontoso and G. Soyez, *Lund multiplicity in QCD jets*, *JHEP* **04** (2023) 104 [arXiv:2212.05076] [INSPIRE].

[36] R. Medves, A. Soto-Ontoso and G. Soyez, *Lund and Cambridge multiplicities for precision physics*, *JHEP* **10** (2022) 156 [arXiv:2205.02861] [INSPIRE].

[37] D. de Florian and M. Grazzini, *The Back-to-back region in e^+e^- energy-energy correlation*, *Nucl. Phys. B* **704** (2005) 387 [hep-ph/0407241] [INSPIRE].

[38] T. Becher and M.D. Schwartz, *A precise determination of α_s from LEP thrust data using effective field theory*, *JHEP* **07** (2008) 034 [arXiv:0803.0342] [INSPIRE].

[39] R. Abbate et al., *Thrust at N^3LL with Power Corrections and a Precision Global Fit for $\alpha_s(mZ)$*, *Phys. Rev. D* **83** (2011) 074021 [arXiv:1006.3080] [INSPIRE].

[40] Y.-T. Chien and M.D. Schwartz, *Resummation of heavy jet mass and comparison to LEP data*, *JHEP* **08** (2010) 058 [arXiv:1005.1644] [INSPIRE].

[41] P.F. Monni, T. Gehrmann and G. Luisoni, *Two-Loop Soft Corrections and Resummation of the Thrust Distribution in the Dijet Region*, *JHEP* **08** (2011) 010 [arXiv:1105.4560] [INSPIRE].

[42] T. Becher and G. Bell, *NNLL Resummation for Jet Broadening*, *JHEP* **11** (2012) 126 [arXiv:1210.0580] [INSPIRE].

[43] A.H. Hoang, D.W. Kolodrubetz, V. Mateu and I.W. Stewart, *C-parameter distribution at N^3LL' including power corrections*, *Phys. Rev. D* **91** (2015) 094017 [arXiv:1411.6633] [INSPIRE].

[44] A. Banfi, H. McAslan, P.F. Monni and G. Zanderighi, *A general method for the resummation of event-shape distributions in e^+e^- annihilation*, *JHEP* **05** (2015) 102 [arXiv:1412.2126] [INSPIRE].

JHEP03(2025)209

[45] A. Banfi, H. McAslan, P.F. Monni and G. Zanderighi, *The two-jet rate in e^+e^- at next-to-next-to-leading-logarithmic order*, *Phys. Rev. Lett.* **117** (2016) 172001 [arXiv:1607.03111] [INSPIRE].

[46] C. Frye, A.J. Larkoski, M.D. Schwartz and K. Yan, *Precision physics with pile-up insensitive observables*, arXiv:1603.06375 [INSPIRE].

[47] C. Frye, A.J. Larkoski, M.D. Schwartz and K. Yan, *Factorization for groomed jet substructure beyond the next-to-leading logarithm*, *JHEP* **07** (2016) 064 [arXiv:1603.09338] [INSPIRE].

[48] Z. Tulipánt, A. Kardos and G. Somogyi, *Energy-energy correlation in electron-positron annihilation at NNLL + NNLO accuracy*, *Eur. Phys. J. C* **77** (2017) 749 [arXiv:1708.04093] [INSPIRE].

[49] I. Moult and H.X. Zhu, *Simplicity from Recoil: The Three-Loop Soft Function and Factorization for the Energy-Energy Correlation*, *JHEP* **08** (2018) 160 [arXiv:1801.02627] [INSPIRE].

[50] G. Bell, A. Hornig, C. Lee and J. Talbert, *e^+e^- angularity distributions at NNLL′ accuracy*, *JHEP* **01** (2019) 147 [arXiv:1808.07867] [INSPIRE].

[51] A. Banfi, B.K. El-Menoufi and P.F. Monni, *The Sudakov radiator for jet observables and the soft physical coupling*, *JHEP* **01** (2019) 083 [arXiv:1807.11487] [INSPIRE].

[52] M. Procura, W.J. Waalewijn and L. Zeune, *Joint resummation of two angularities at next-to-next-to-leading logarithmic order*, *JHEP* **10** (2018) 098 [arXiv:1806.10622] [INSPIRE].

[53] L. Arpino, A. Banfi and B.K. El-Menoufi, *Near-to-planar three-jet events at NNLL accuracy*, *JHEP* **07** (2020) 171 [arXiv:1912.09341] [INSPIRE].

[54] C.W. Bauer, A.V. Manohar and P.F. Monni, *Disentangling observable dependence in $SCET_I$ and $SCET_{II}$ anomalous dimensions: angularities at two loops*, *JHEP* **07** (2021) 214 [arXiv:2012.09213] [INSPIRE].

[55] A. Kardos, A.J. Larkoski and Z. Trócsányi, *Groomed jet mass at high precision*, *Phys. Lett. B* **809** (2020) 135704 [arXiv:2002.00942] [INSPIRE].

[56] D. Anderle et al., *Groomed jet mass as a direct probe of collinear parton dynamics*, *Eur. Phys. J. C* **80** (2020) 827 [arXiv:2007.10355] [INSPIRE].

[57] C. Duhr, B. Mistlberger and G. Vita, *Four-Loop Rapidity Anomalous Dimension and Event Shapes to Fourth Logarithmic Order*, *Phys. Rev. Lett.* **129** (2022) 162001 [arXiv:2205.02242] [INSPIRE].

[58] M. Dasgupta, B.K. El-Menoufi and J. Helliwell, *QCD resummation for groomed jet observables at NNLL+NLO*, *JHEP* **01** (2023) 045 [arXiv:2211.03820] [INSPIRE].

[59] V.N. Gribov and L.N. Lipatov, *Deep inelastic e p scattering in perturbation theory*, *Sov. J. Nucl. Phys.* **15** (1972) 438 [INSPIRE].

[60] Y.L. Dokshitzer, *Calculation of the Structure Functions for Deep Inelastic Scattering and e^+e^- Annihilation by Perturbation Theory in Quantum Chromodynamics*, *Sov. Phys. JETP* **46** (1977) 641 [INSPIRE].

[61] G. Altarelli and G. Parisi, *Asymptotic Freedom in Parton Language*, *Nucl. Phys. B* **126** (1977) 298 [INSPIRE].

[62] W. Furmanski and R. Petronzio, *Singlet Parton Densities Beyond Leading Order*, *Phys. Lett. B* **97** (1980) 437 [INSPIRE].

[63] G. Curci, W. Furmanski and R. Petronzio, *Evolution of Parton Densities Beyond Leading Order: The Nonsinglet Case*, *Nucl. Phys. B* **175** (1980) 27 [INSPIRE].

JHEP03(2025)209

[64] A. Jain, M. Procura and W.J. Waalewijn, *Parton Fragmentation within an Identified Jet at NNLL*, *JHEP* **05** (2011) 035 [arXiv:1101.4953] [INSPIRE].

[65] S. Alioli and J.R. Walsh, *Jet Veto Clustering Logarithms Beyond Leading Order*, *JHEP* **03** (2014) 119 [arXiv:1311.5234] [INSPIRE].

[66] H.-M. Chang, M. Procura, J. Thaler and W.J. Waalewijn, *Calculating Track-Based Observables for the LHC*, *Phys. Rev. Lett.* **111** (2013) 102002 [arXiv:1303.6637] [INSPIRE].

[67] M. Ritzmann and W.J. Waalewijn, *Fragmentation in Jets at NNLO*, *Phys. Rev. D* **90** (2014) 054029 [arXiv:1407.3272] [INSPIRE].

[68] M. Dasgupta, F. Dreyer, G.P. Salam and G. Soyez, *Small-radius jets to all orders in QCD*, *JHEP* **04** (2015) 039 [arXiv:1411.5182] [INSPIRE].

[69] A. Banfi et al., *Jet-vetoed Higgs cross section in gluon fusion at N^3LO+NNLL with small-R resummation*, *JHEP* **04** (2016) 049 [arXiv:1511.02886] [INSPIRE].

[70] M. Dasgupta, F.A. Dreyer, G.P. Salam and G. Soyez, *Inclusive jet spectrum for small-radius jets*, *JHEP* **06** (2016) 057 [arXiv:1602.01110] [INSPIRE].

[71] Z.-B. Kang, F. Ringer and I. Vitev, *The semi-inclusive jet function in SCET and small radius resummation for inclusive jet production*, *JHEP* **10** (2016) 125 [arXiv:1606.06732] [INSPIRE].

[72] L.J. Dixon, I. Moult and H.X. Zhu, *Collinear limit of the energy-energy correlator*, *Phys. Rev. D* **100** (2019) 014009 [arXiv:1905.01310] [INSPIRE].

[73] H. Chen, I. Moult and H.X. Zhu, *Quantum Interference in Jet Substructure from Spinning Gluons*, *Phys. Rev. Lett.* **126** (2021) 112003 [arXiv:2011.02492] [INSPIRE].

[74] H. Chen, I. Moult and H.X. Zhu, *Spinning gluons from the QCD light-ray OPE*, *JHEP* **08** (2022) 233 [arXiv:2104.00009] [INSPIRE].

[75] M. Dasgupta and B.K. El-Menoufi, *Dissecting the collinear structure of quark splitting at NNLL*, *JHEP* **12** (2021) 158 [arXiv:2109.07496] [INSPIRE].

[76] Y. Li et al., *Extending Precision Perturbative QCD with Track Functions*, *Phys. Rev. Lett.* **128** (2022) 182001 [arXiv:2108.01674] [INSPIRE].

[77] H. Chen, I. Moult, J. Sandor and H.X. Zhu, *Celestial blocks and transverse spin in the three-point energy correlator*, *JHEP* **09** (2022) 199 [arXiv:2202.04085] [INSPIRE].

[78] H. Chen et al., *Collinear Parton Dynamics Beyond DGLAP*, arXiv:2210.10061 [INSPIRE].

[79] X. Liu and H.X. Zhu, *Nucleon Energy Correlators*, *Phys. Rev. Lett.* **130** (2023) 091901 [arXiv:2209.02080] [INSPIRE].

[80] W. Chen et al., *NNLL resummation for projected three-point energy correlator*, *JHEP* **05** (2024) 043 [arXiv:2307.07510] [INSPIRE].

[81] M. van Beekveld et al., *Collinear fragmentation at NNLL: generating functionals, groomed correlators and angularities*, *JHEP* **05** (2024) 093 [arXiv:2307.15734] [INSPIRE].

[82] K. Lee and I. Moult, *Energy Correlators Taking Charge*, arXiv:2308.00746 [INSPIRE].

[83] K. Lee, A. Pathak, I.W. Stewart and Z. Sun, *Nonperturbative Effects in Energy Correlators: From Characterizing Confinement Transition to Improving α_s Extraction*, *Phys. Rev. Lett.* **133** (2024) 231902 [arXiv:2405.19396] [INSPIRE].

[84] H. Chen, P.F. Monni, Z. Xu and H.X. Zhu, *Scaling Violation in Power Corrections to Energy Correlators from the Light-Ray Operator Product Expansion*, *Phys. Rev. Lett.* **133** (2024) 231901 [arXiv:2406.06668] [INSPIRE].

JHEP03(2025)209

[85] K. Hamilton, P. Nason, E. Re and G. Zanderighi, *NNLOPS simulation of Higgs boson production*, *JHEP* **10** (2013) 222 [arXiv:1309.0017] [INSPIRE].

[86] S. Alioli et al., *Matching Fully Differential NNLO Calculations and Parton Showers*, *JHEP* **06** (2014) 089 [arXiv:1311.0286] [INSPIRE].

[87] S. Höche, Y. Li and S. Prestel, *Drell-Yan lepton pair production at NNLO QCD with parton showers*, *Phys. Rev. D* **91** (2015) 074015 [arXiv:1405.3607] [INSPIRE].

[88] P.F. Monni et al., *MiNNLO$_{PS}$: a new method to match NNLO QCD to parton showers*, *JHEP* **05** (2020) 143 [*Erratum ibid.* **02** (2022) 031] [arXiv:1908.06987] [INSPIRE].

[89] P.F. Monni, E. Re and M. Wiesemann, *MiNNLO$_{PS}$: optimizing* $2 \to 1$ *hadronic processes*, *Eur. Phys. J. C* **80** (2020) 1075 [arXiv:2006.04133] [INSPIRE].

[90] S. Alioli et al., *Matching NNLO predictions to parton showers using N3LL color-singlet transverse momentum resummation in geneva*, *Phys. Rev. D* **104** (2021) 094020 [arXiv:2102.08390] [INSPIRE].

[91] J.M. Campbell and E.W.N. Glover, *Double unresolved approximations to multiparton scattering amplitudes*, *Nucl. Phys. B* **527** (1998) 264 [hep-ph/9710255] [INSPIRE].

[92] S. Catani and M. Grazzini, *Collinear factorization and splitting functions for next-to-next-to-leading order QCD calculations*, *Phys. Lett. B* **446** (1999) 143 [hep-ph/9810389] [INSPIRE].

[93] Z. Bern, L.J. Dixon, D.C. Dunbar and D.A. Kosower, *One loop n point gauge theory amplitudes, unitarity and collinear limits*, *Nucl. Phys. B* **425** (1994) 217 [hep-ph/9403226] [INSPIRE].

[94] Z. Bern and G. Chalmers, *Factorization in one loop gauge theory*, *Nucl. Phys. B* **447** (1995) 465 [hep-ph/9503236] [INSPIRE].

[95] D.A. Kosower, *All order collinear behavior in gauge theories*, *Nucl. Phys. B* **552** (1999) 319 [hep-ph/9901201] [INSPIRE].

[96] D.A. Kosower and P. Uwer, *One loop splitting amplitudes in gauge theory*, *Nucl. Phys. B* **563** (1999) 477 [hep-ph/9903515] [INSPIRE].

[97] G.F.R. Sborlini, D. de Florian and G. Rodrigo, *Double collinear splitting amplitudes at next-to-leading order*, *JHEP* **01** (2014) 018 [arXiv:1310.6841] [INSPIRE].

[98] M. van Beekveld et al., *Two-loop anomalous dimensions for small-R jet versus hadronic fragmentation functions*, *JHEP* **07** (2024) 239 [arXiv:2402.05170] [INSPIRE].

[99] S. Catani, B.R. Webber and G. Marchesini, *QCD coherent branching and semiinclusive processes at large x*, *Nucl. Phys. B* **349** (1991) 635 [INSPIRE].

[100] S. Catani, D. De Florian and M. Grazzini, *Soft-gluon effective coupling and cusp anomalous dimension*, *Eur. Phys. J. C* **79** (2019) 685 [arXiv:1904.10365] [INSPIRE].

[101] S. Frixione and B.R. Webber, *Matching NLO QCD computations and parton shower simulations*, *JHEP* **06** (2002) 029 [hep-ph/0204244] [INSPIRE].

[102] P. Nason, *A new method for combining NLO QCD with shower Monte Carlo algorithms*, *JHEP* **11** (2004) 040 [hep-ph/0409146] [INSPIRE].

[103] K. Hamilton et al., *Matching and event-shape NNDL accuracy in parton showers*, *JHEP* **03** (2023) 224 [*Erratum ibid.* **11** (2023) 060] [arXiv:2301.09645] [INSPIRE].

[104] N. Lavesson and L. Lönnblad, *Extending CKKW-merging to One-Loop Matrix Elements*, *JHEP* **12** (2008) 070 [arXiv:0811.2912] [INSPIRE].

JHEP03(2025)209

[105] S. Hoeche, F. Krauss, M. Schonherr and F. Siegert, *QCD matrix elements + parton showers: The NLO case*, *JHEP* **04** (2013) 027 [arXiv:1207.5030] [INSPIRE].

[106] T. Gehrmann et al., *NLO QCD matrix elements + parton showers in $e^+e^- \to$ hadrons*, *JHEP* **01** (2013) 144 [arXiv:1207.5031] [INSPIRE].

[107] R. Frederix and S. Frixione, *Merging meets matching in MC@NLO*, *JHEP* **12** (2012) 061 [arXiv:1209.6215] [INSPIRE].

[108] S. Plätzer, *Controlling inclusive cross sections in parton shower + matrix element merging*, *JHEP* **08** (2013) 114 [arXiv:1211.5467] [INSPIRE].

[109] L. Lönnblad and S. Prestel, *Merging Multi-leg NLO Matrix Elements with Parton Showers*, *JHEP* **03** (2013) 166 [arXiv:1211.7278] [INSPIRE].

[110] G.P. Salam and J. Rojo, *A Higher Order Perturbative Parton Evolution Toolkit (HOPPET)*, *Comput. Phys. Commun.* **180** (2009) 120 [arXiv:0804.3755] [INSPIRE].

[111] Y.L. Dokshitzer, G.D. Leder, S. Moretti and B.R. Webber, *Better jet clustering algorithms*, *JHEP* **08** (1997) 001 [hep-ph/9707323] [INSPIRE].

[112] M. Wobisch and T. Wengler, *Hadronization corrections to jet cross-sections in deep inelastic scattering*, in the proceedings of the *Workshop on Monte Carlo Generators for HERA Physics (Plenary Starting Meeting)*, Hamburg, Germany, April 27–30 (1998) [hep-ph/9907280] [INSPIRE].

[113] M. Cacciari, G.P. Salam and G. Soyez, *FastJet User Manual*, *Eur. Phys. J. C* **72** (2012) 1896 [arXiv:1111.6097] [INSPIRE].

[114] A. Banfi, G.P. Salam and G. Zanderighi, *Infrared safe definition of jet flavor*, *Eur. Phys. J. C* **47** (2006) 113 [hep-ph/0601139] [INSPIRE].

[115] A. Banfi, G.P. Salam and G. Zanderighi, *Accurate QCD predictions for heavy-quark jets at the Tevatron and LHC*, *JHEP* **07** (2007) 026 [arXiv:0704.2999] [INSPIRE].

[116] M. Czakon, A. Mitov and R. Poncelet, *Infrared-safe flavoured anti-k_T jets*, *JHEP* **04** (2023) 138 [arXiv:2205.11879] [INSPIRE].

[117] R. Gauld, A. Huss and G. Stagnitto, *Flavor Identification of Reconstructed Hadronic Jets*, *Phys. Rev. Lett.* **130** (2023) 161901 [*Erratum ibid.* **132** (2024) 159901] [arXiv:2208.11138] [INSPIRE].

[118] F. Caola et al., *Flavored jets with exact anti-kt kinematics and tests of infrared and collinear safety*, *Phys. Rev. D* **108** (2023) 094010 [arXiv:2306.07314] [INSPIRE].

[119] S. Caletti, A.J. Larkoski, S. Marzani and D. Reichelt, *Practical jet flavour through NNLO*, *Eur. Phys. J. C* **82** (2022) 632 [arXiv:2205.01109] [INSPIRE].

[120] S. Caletti, A.J. Larkoski, S. Marzani and D. Reichelt, *A fragmentation approach to jet flavor*, *JHEP* **10** (2022) 158 [arXiv:2205.01117] [INSPIRE].

[121] A.J. Larkoski, *Flavor factorization at two-loops*, *Eur. Phys. J. C* **84** (2024) 1131 [arXiv:2402.06735] [INSPIRE].

[122] A.J. Larkoski and D. Neill, *Flavor fragmentation function factorization*, *JHEP* **01** (2024) 119 [arXiv:2310.01486] [INSPIRE].

JHEP03(2025)209